AD NUMBER: AD0525987
CLASSIFICATION CHANGES
TO: Unclassified
FROM: Confidential
AUTHORITY
Per DoDD 5200.1 dtd 31 Dec 1981

AD NUMBER: AD0525987
CLASSIFICATION CHANGES
TO: Confidential
FROM: Secret
AUTHORITY
Per DoDd 5200.1 dtd 31 Dec 1975

GENERAL DECLASSIFICATION SCHEDULE

IN ACCORDANCE WITH
DOD 5200.1-R & EXECUTIVE ORDER 11652

SECURITY MARKING

The classified or limited status of this report applies to each page, unless otherwise marked.
Separate page printouts MUST be marked accordingly.

THIS DOCUMENT CONTAINS INFORMATION AFFECTING THE NATIONAL DEFENSE OF THE UNITED STATES WITHIN THE MEANING OF THE ESPIONAGE LAWS, TITLE 18, U.S.C., SECTIONS 793 AND 794. THE TRANSMISSION OR THE REVELATION OF ITS CONTENTS IN ANY MANNER TO AN UNAUTHORIZED PERSON IS PROHIBITED BY LAW.

NOTICE: When government or other drawings, specifications or other data are used for any purpose other than in connection with a definitely related government procurement operation, the U. S. Government thereby incurs no responsibility, nor any obligation whatsoever; and the fact that the Government may have formulated, furnished, or in any way supplied the said drawings, specifications, or other data is not to be regarded by implication or otherwise as in any manner licensing the holder or any other person or corporation, or conveying any rights or permission to manufacture, use or sell any patented invention that may in any way be related thereto.

~~SECRET~~

D180-15330-1

ISSUE NO. 37

DESIGN OF AIRCRAFT CONTROL SURFACES LOW RADAR CROSS SECTION (U)

MAY 1973

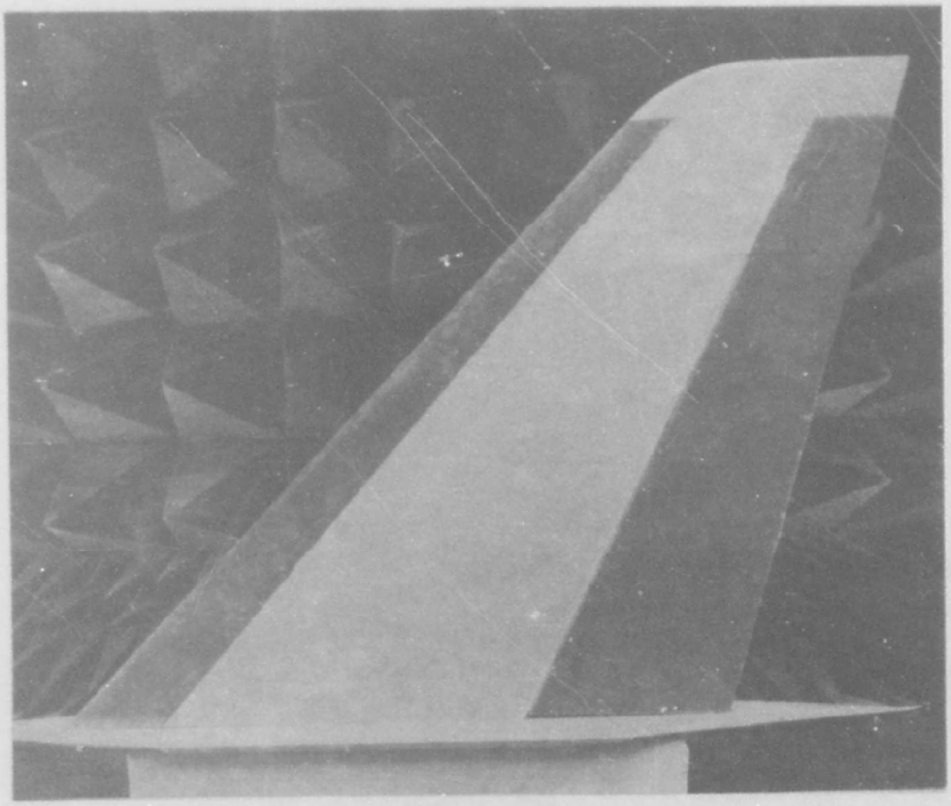

PREPARED FOR: THE OFFICE OF NAVAL RESEARCH
AERONAUTICS PROGRAMS
ARLING, VIRGINIA
CONTRACT N00014-72-C-0303/NR215-184

SECRET CLASSIFIED BY: DIRECTOR, NAVAL APPLICATIONS & ANALYSIS DIVISION
SUBJECT TO GENERAL DECLASSIFICATION SCHEDULE OF
EXECUTIVE ORDER 11652. AUTOMATICALLY DOWNGRADED
AT TWO YEAR INTERVALS AND DECLASSIFIED ON 31 DEC. 1981

RESEARCH & ENGINEERING DIVISION
BOEING AEROSPACE COMPANY
(A DIVISION OF THE BOEING COMPANY)
SEATTLE, WASHINGTON 98124

~~SECRET~~

UNCLASSIFIED
Security Classification

DOCUMENT CONTROL DATA - R&D

(Security classification of title, body of abstract and indexing annotation must be entered when the overall report is classified).

1. ORIGINATING ACTIVITY (Corporate author)
The Boeing Aerospace Company
Seattle, Washington 98124

2a. REPORT SECURITY CLASSIFICATION
[redacted]

2b. GROUP
GDS

3. REPORT TITLE
Design of Aircraft Control Surface
Low Radar Cross Section

4. DESCRIPTIVE NOTES (Types of report and inclusive dates)
Annual Technical Report

5. AUTHORS (First name, middle initial, last name)
John D. Kelly
Gordon A. Taylor

6. REPORT DATE
May 1, 1973

7a. TOTAL NO. OF PAGES
64

7b. NO. OF REFS
5

8a. CONTRACT OR GRANT NO.
N00014-72-C-0303/NR215-184

b.

c.

d.

9a. ORIGINATOR'S REPORT NUMBERS
D180-15330-1

9b. OTHER REPORT NO(S) (Any other numbers that may be assigned this report)

10. DISTRIBUTION STATEMENT
Qualified Requestors may obtain a copy of this report from DDC.

11. SUPPLEMENTARY NOTES

12. SPONSORING MILITARY ACTIVITY
Office of Naval Research
Arlington, Virginia 22217

13. ABSTRACT

This report describes the technical details of a research program to examine the radar cross section (RCS) from a typical aircraft control surface. The nature and extent of the RCS was determined for a vertical tail structure and techniques for reducing this RCS examined.

DD FORM 1 NOV 68 1473
D1 4802 1030 ORIG. 3/71
PART 1 OF 3

UNCLASSIFIED
Security Classification

14. KEY WORDS	LINK A		LINK B		LINK C	
	ROLE	WT	ROLE	WT	ROLE	2 T
Radar Cross Section (RCS)						
Radar Absorber Materials						
Travelling Waves						

~~SECRET~~

D180-15330-1

ISSUE No. 37

ANNUAL TECHNICAL REPORT

DESIGN OF AIRCRAFT CONTROL SURFACES LOW RADAR CROSS SECTION (U)

MAY 1973

PREPARED FOR:
THE OFFICE OF NAVAL RESEARCH
AERONAUTICS PROGRAMS
ARLINGTON, VIRGINIA
CONTRACT N00014-72-C-0303/NR215-184

SECRET CLASSIFIED BY:
DIRECTOR, NAVAL APPLICATIONS & ANALYSIS DIVISION
SUBJECT TO GENERAL DECLASSIFICATION SCHEDULE
OF EXECUTIVE ORDER 11652. AUTOMATICALLY DOWN-
GRADED AT TWO YEAR INTERVALS & DECLASSIFIED ON
31 DECEMBER 1981

RESEARCH & ENGINEERING DIVISION
BOEING AEROSPACE COMPANY
(A DIVISION OF THE BOEING COMPANY)
SEATTLE, WASHINGTON 98124

~~SECRET~~

TABLE OF CONTENTS (U)

ILLUSTRATIONS

ILLUSTRATIONS (Cont)

1.0 INTRODUCTION

(S) Early studies into the radar cross section (RCS) of airplanes have identified the following components as major RCS contributors: engine inlets, exhaust nozzles, crew compartments, radar antennas and the external stores. Subsequently, these were followed by studies which addressed the problem of reducing the level of RCS from these components. Presently the studies have demonstrated that an airplane RCS of one square meter can be realized, for the nose sector of the aircraft. A one square meter RCS has been selected as a nominal design goal for various military airplanes and reflects a design approach where the RCS considerations do not signficantly influence the configuration during the preliminary design stages. Therefore, a one square meter RCS does not represent either a minimum or the optimum level that is achievable for a given aircraft.

(S) A recent study sponsored by the Office of Naval Research (ONR) was conducted by the Boeing Company to determine what level of RCS is practical for an advanced fighter-attack airplane designed for low RCS. A supersonic fighter-attack airplane which had some desirable low RCS features was selected as a baseline for this study. The RCS attainable by retro-fitting this configuration ("reduced" RCS baseline) was determined and compared with the RCS achieved by designing a new, "low RCS" configuration to perform identical missions. The cost and mission performance factors were also compared for the baseline, "reduced" RCS baseline and "low-RCS" configurations. A RCS of .05 square meters in the forward sector was shown to be practical for the "low RCS" configuration and a 0.25 square meter RCS for the retrofit baseline. Whereas the RCS was 4.6 square meters for the baseline configuration. The "low RCS" level was achieved with no significant cost or performance penalties by employing a coordinated interdisciplinary design approach between RCS, aerodynamics, propulsion, and other related technologies.

(S) In order to achieve this level of RCS it was assumed that the forward sector RCS from the airframe (excluding the previously mentioned contributors) could be controlled to a level near .01 square meters. Previous studies of airframe RCS have been based almost exclusively on scaled model measurements and calculations based upon geometrical optics type of scattering. Scaled models have not included the surface details such as rudders, flaps, elevators, etc. These details have been assumed to be insignificant for RCS levels above one square meters. However, the previous studies on low RCS bodies at Boeing have shown that surface details and shape can significantly influence the RCS for levels below 0.1 square meter. Furthermore, it was determined that the scattering from travelling waves can be substantial for low levels of RCS. Travelling waves are not thoroughly understood on aircraft shapes and are not allowed for in the geometrical optics scattering theories that are often applied for calculating the RCS of an airframe.

(U) The research study described in this report was undertaken to obtain a preliminary understanding of the scattering nature from the control surfaces on an airframe and to investigate practical methods for reducing the RCS. The vertical tail was selected as a representative airplane component which contains the type of control surface of concern, namely the rudder. A combination of analytical and experimental studies was used to examine a vertical tail configuration. The data and analyses on the tail are generally applicable to other control surfaces on the aircraft.

(U) Full-scale models of the tail were constructed and tested. Techniques were examined to reduce the RCS from the tail at the forward, aft and broadside aspects from 2-12 GHz. Structural radar absorbing materials were emphasized for RCS reduction to similiar weight. New materials and techniques developed during this study were tested on the full-scale models and their RCS reduction potential established.

(C) The program established the nature and extent of the RCS from a typical airframe component incorporating control surfaces and developed practical techniques for control of the airframe RCS consistent with an .01 square meter level over the nose and tail sectors. This research has examined a previously unstudied problem and is directly applicable to airplane design where low RCS is a design parameter.

2.0 SUMMARY

(S) The airframe (wings, tail, fuselage) has not been considered a major radar cross section (RCS) contributor of interest for current military airplanes. Present airplanes have had little RCS control applied during their initial design with a radar cross section design goal of one square meter considered to be a typical target value for the nose sector. In general, it has been assumed that the airframe will not substantially influence the RCS in the nose sector at this level.

(U) A recent research program conducted by the Boeing Company, and funded by the Office of Naval Research, showed that the RCS, from an advanced fighter-attack airplane can be controlled to 0.05 square meters in the forward sector, if an interdisciplinary design approach is taken during the initial stages of the aircraft design. Fundamental to attaining this low RCS design goal is the control of the airframe RCS to a level of .01 square meters. This RCS level was judged to be attainable but it was recognized that a more detailed study of the airframe was required, particularly of the discontinuties associated with the control surfaces (rudder, flaps, elevators, etc).

(U) The key elements of this study were designed to accomplish the following:

- o determine the nature and extent of the RCS from a typical airframe component incorporating a control surface (a vertical tail)
- o determine practical methods for reducing the RCS from the vertical tail for the forward, aft, and broadside sectors
- o develop preliminary design data and drawings for a vertical tail exhibiting low RCS.

(S) The majority of the experimental work for the study was performed on two, full-scale vertical tail models: 1) A "smooth" model conforming to the external lines of the tail but with no moveable rudder or surface details, and 2) A "detailed" model with moveable rudder and surface details (rudder hinge gap, panel join lines, etc). The RCS was measured for these models from 2-12 GHz at various attitudes. The "detailed" model exhibited a much larger RCS than the "smooth" model due to a large travelling wave contribution for the travelling wave. Average RCS levels exceeding 0.1 square meters were observed for the detailed model in the forward and aft sectors. These levels are significantly greater than those measured for "smooth" surface models that are commonly used in RCS tests.

(S) The reduction of the RCS for the forward and aft sector of the tail was accomplished by applying the following: 1) Installing a structural, magnetic absorber as the trailing edge surface, 2) Installing a metallic rudder hinge fairing, 3) Controlling all surface

(S)
discontinuties (panel join lines, rivets, etc.). The structural magnetic absorber was developed specifically for this study and is a new type of absorber material. These treatments can provide a RCS for the forward and aft sectors below .01 square meters.

(S) The RCS for the broadside sector was reduced by installing either radar transmissive or circuit analog radar absorber side panels. The resulting RCS was reduced from 100 square meters to 10 to 20 square meters, depending on the frequency. However, each of the broadside RCS reduction techniques, incorporated, resulted in a substantial increase in the RCS for the forward and aft sector to above 0.1 square meters. Achieving compatibility of broadside sector RCS reduction for the tail with a low RCS for the forward and aft sector will require additional study.

(S) A preliminary design for a vertical tail was developed which includes:

- structural magnetic absorber as a trailing edge surface
- metal rudder hinge fairing
- surface detail control
- structural specular absorber side panels and leading edge fairing

(S) The results from tests and analysis performed during this program indicate that an airframe can be designed to satisfy a .01 square meter RCS in the forward and aft sectors. This level of radar cross section is consistent with a RCS design goal of 0.05 square meters for an aircraft.

3.0 PROGRAM DATA AND ANALYSES

(U) The objectives of this program were to identify the nature and extent of the RCS from typical airframe control surfaces and to determine practical methods for reducing their RCS in the forward, aft and broadside sectors. The objectives of this study were achieved by performing a series of related tests and analyses designed to: 1) identify the magnitude of the RCS from a representative control surface, 2) resolve the scattering sources, 3) determine practical means for reducing the RCS, 4) develop a preliminary design for a low RCS vertical tail, and 5) relate the program results to overall airplane low RCS design methods. Experimental verification was obtained for the various RCS reduction methods studied and the RCS for the preliminary design was established by full-scale measurements using prototype materials.

3.1 Baseline RCS Measurements

(U) A vertical tail geometry was selected as a baseline configuration for this study. The tail was chosen as it is small and therefore simplifies full-scale modeling. A vertical tail is representative of a typical airframe component containing a control surface, namely the rudder. The results of this study on the tail are generally applicable to other control surfaces on the airframe. The tail used in the study was designed by Boeing for a supersonic-light-weight fighter configuration. The general size and shape of this tail is comparable to those on the F-14 and F-15 fighters which represent the current state-of-the-art in this type of aircraft.

(C) Two full-scale models were built of the tail. One model was "smooth" and had no gaps, discontinuities or moveable rudder surface. The second model was built using frame and skin construction and includes the moveable rudder. This is referred to as the "detailed" model to indicate the presence of surface discontinuities and details. The overall dimensions of these models are shown in Figure 3.1 and photographs of the models in Figures 3.2 and 3.3. Measurements were made on these two models to determine their RCS signature at 2.0, 4.0 and 10.0 GHz. The RCS at these frequencies characterize the RCS across the 2-12 GHz microwave band. This frequency band is considered typical of the major threat bands for which RCS is important. The measurement coordinate system used throughout this program is shown in Figure 3.4.

(U) Measured data for the two tail models are compared based on the median RCS about both nose-on and tail-on to the aircraft. The median value is the level which the RCS exceeds for one-half of the angular sector. The median is commonly used to smooth the highly oscillatory measured RCS data and simplifies the data analysis. The RCS data were taken for conic angles of 0°, +10°, +20° and +30° with 0° being the aircraft's yaw plane. The conic angle is defined as follows: The axis of rotation for the model is normal to the aircraft yaw plane. A positive conic "pattern" is obtained by

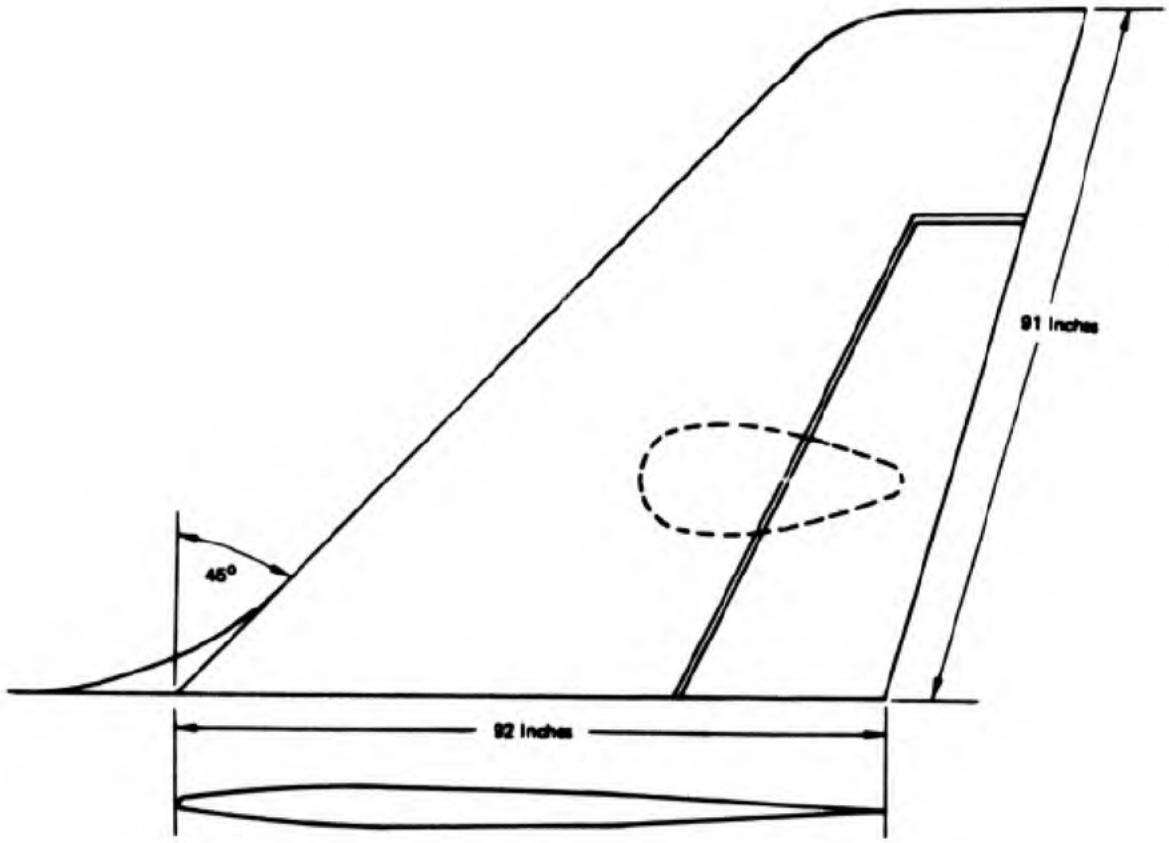

Figure 3.1: Vertical Tail Geometry (U)

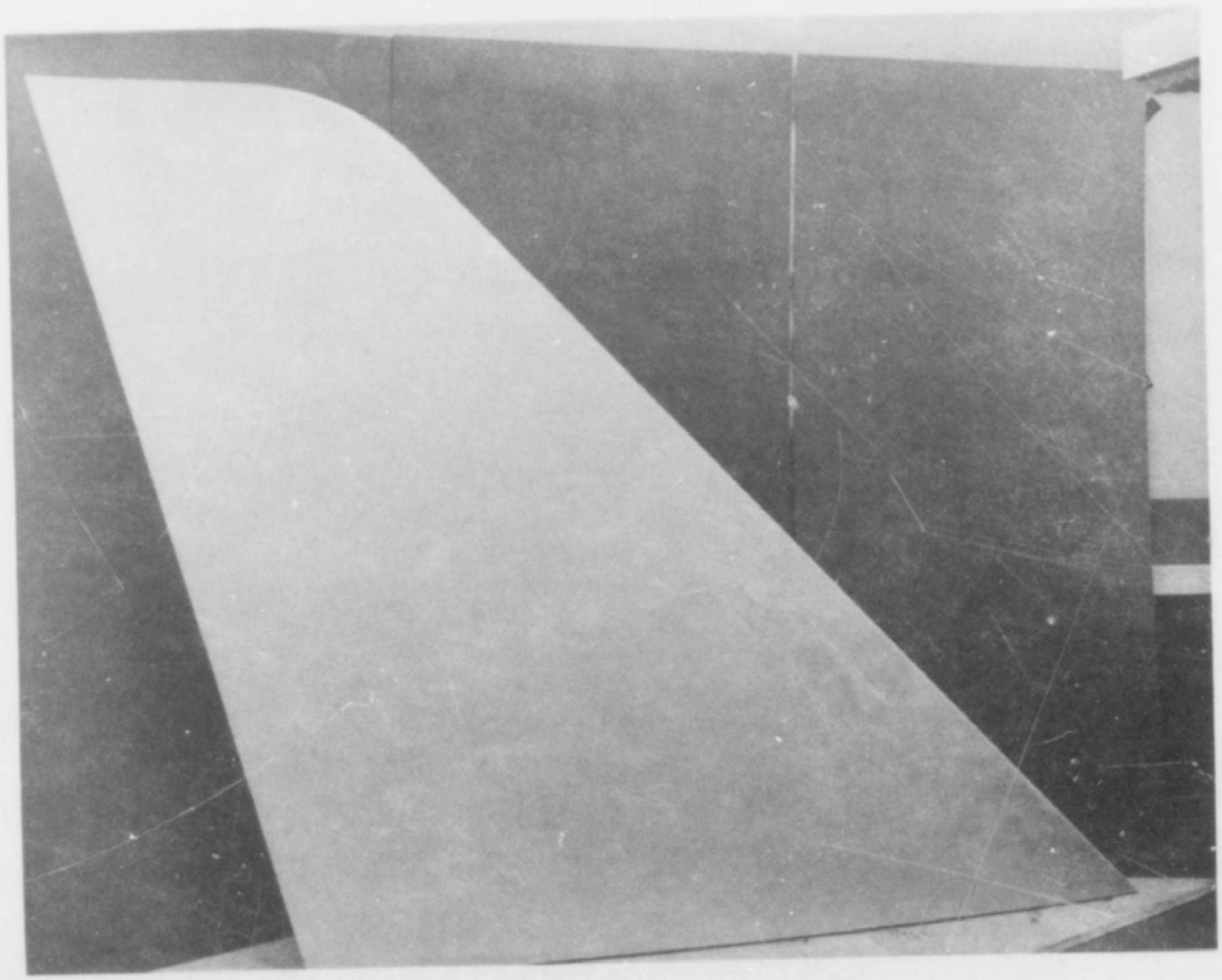

Figure 3-2: Smooth Model (U)

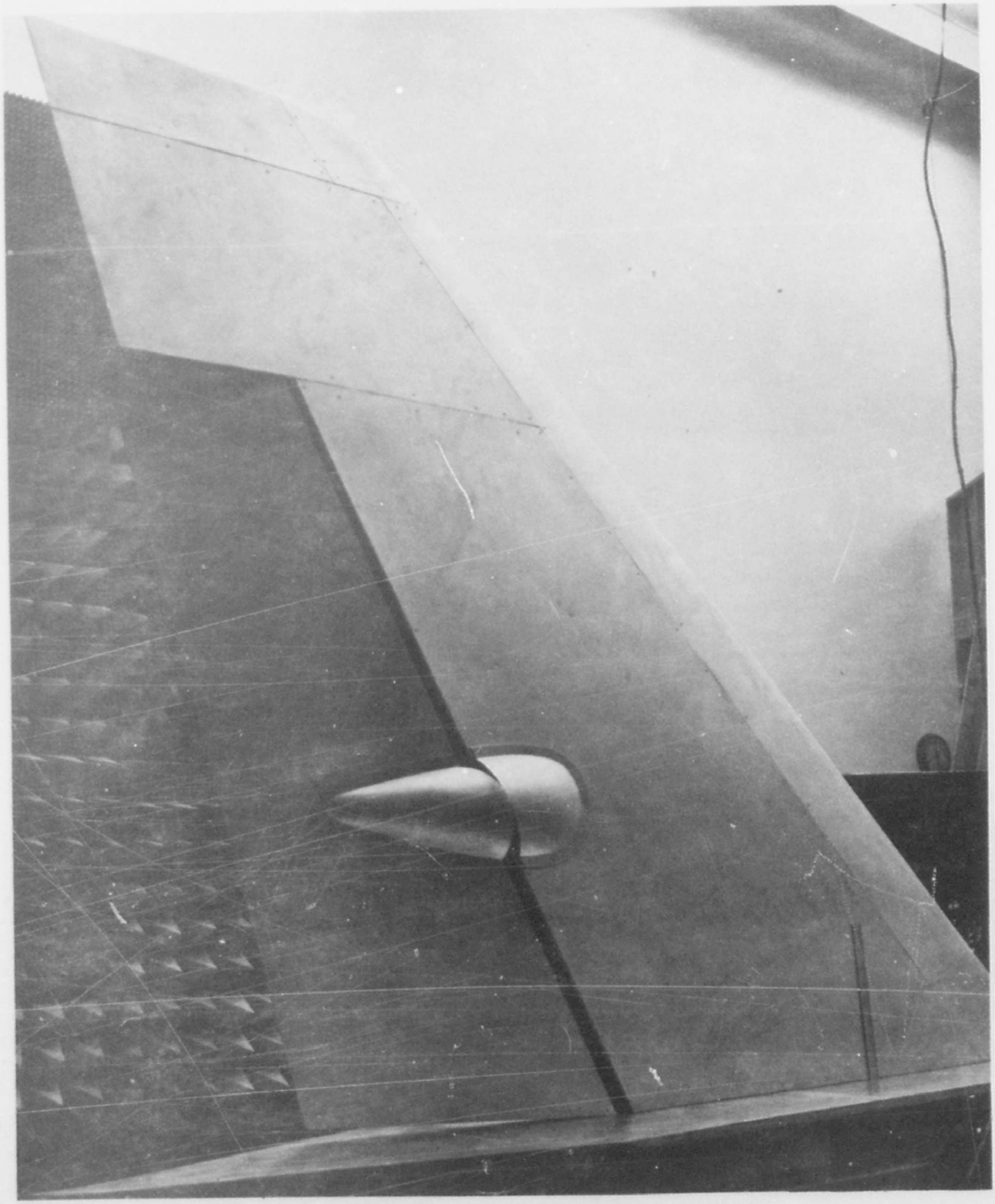

Figure 3.3: Detailed Model (U)

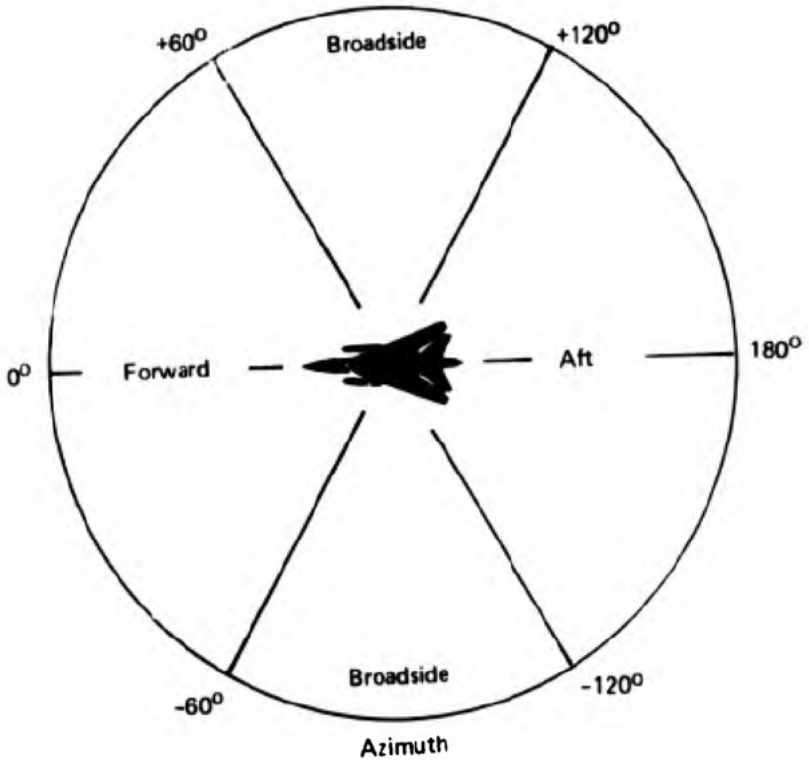

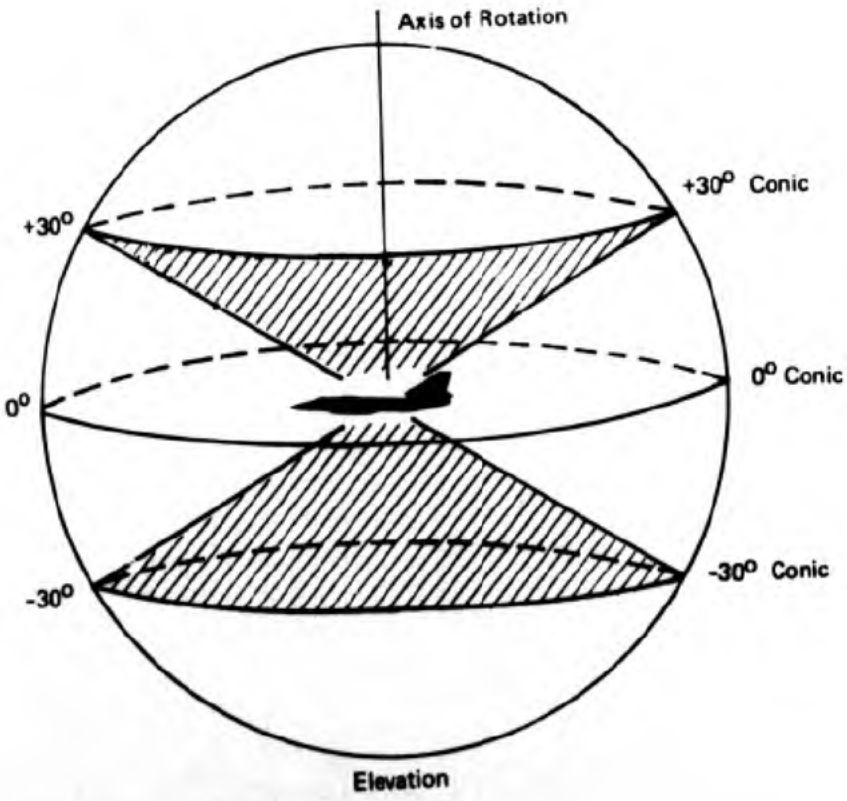

Figure 3.4: Measurement Coordinate System (U)

tilting the axis of rotation forward (towards the illuminating radar) through an angle equal to the conic angle and rotating the model about the previously defined axis of rotation. Therefore at positive conic angles the upper portion of the model is always in view.

(C) Figure 3.5 shows the median RCS in the forward sector for both the "smooth" and the "detailed" models at 2, 4 and 10 GHz, for both vertical and horizontal polarization. Figure 3.6 is a similar data set for the aft sector. The 0, +10, +20 and +30 degree conic angle RCS is shown in each figure. These data show that there are no substantial differences in the RCS for the "smooth" model between vertical and horizontal polarizations. Furthermore, the level of RCS is generally below .01 square meters. The "detailed" model however, shows a higher RCS at horizontal polarization and is near 0.1 square meter at certain angles. This predominance of the horizontally polarized backscatter is a clear indication of the presence of travelling waves along the surface of the tail.

(U) Travelling waves can propagate if the electric field is normal to the metallic surface of the body. This corresponds to a horizontal polarized electric field for a vertical tail structure. The fact that the "detailed" model has a substantial travelling wave RCS is attributed to the large number of discontinuties along the body which perturbs their propagation and thereby reflect some of the wave energy. The "smooth" tail model will primarily reflect the travelling wave from the trailing edge.

3.2 RCS Diagnosis

(C) The location of the reflection points for the travelling waves propagating along the tail were determined by a series of diagnostic tests on a simplified model using the Boeing Short Pulse Range. This facility can generate pulses on the order of 1 nanosecond which enables the spatial resolution of scattering sources to within less than one foot. This capability is shown schematically in Figure 3.7. The results of these tests clearly identified the rudder hinge area, panel join lines, and the trailing edge as RCS contributors. The installation of reflective fairings over the hinge and panel discontinuties effectively eliminated the RCS from these items. Further RCS reduction was achieved by installing a magnetic absorber along the trailing edge of the rudder and tail. This material serves to attenuate the travelling wave prior to their reflection at the trailing edge. A similar treatment to the leading edge was less effective as the untreated curved leading edge fairing is a more suitable termination to travelling waves that are launched from near tail-on aspects.

(C) The rudder actuator fairing was a suspected RCS contributor. Diagnosis using the Short Pulse Range revealed that this was not the case and in fact the fairing could actually provide a small reduction in RCS at forward aspect angles. This is due to the shape of the

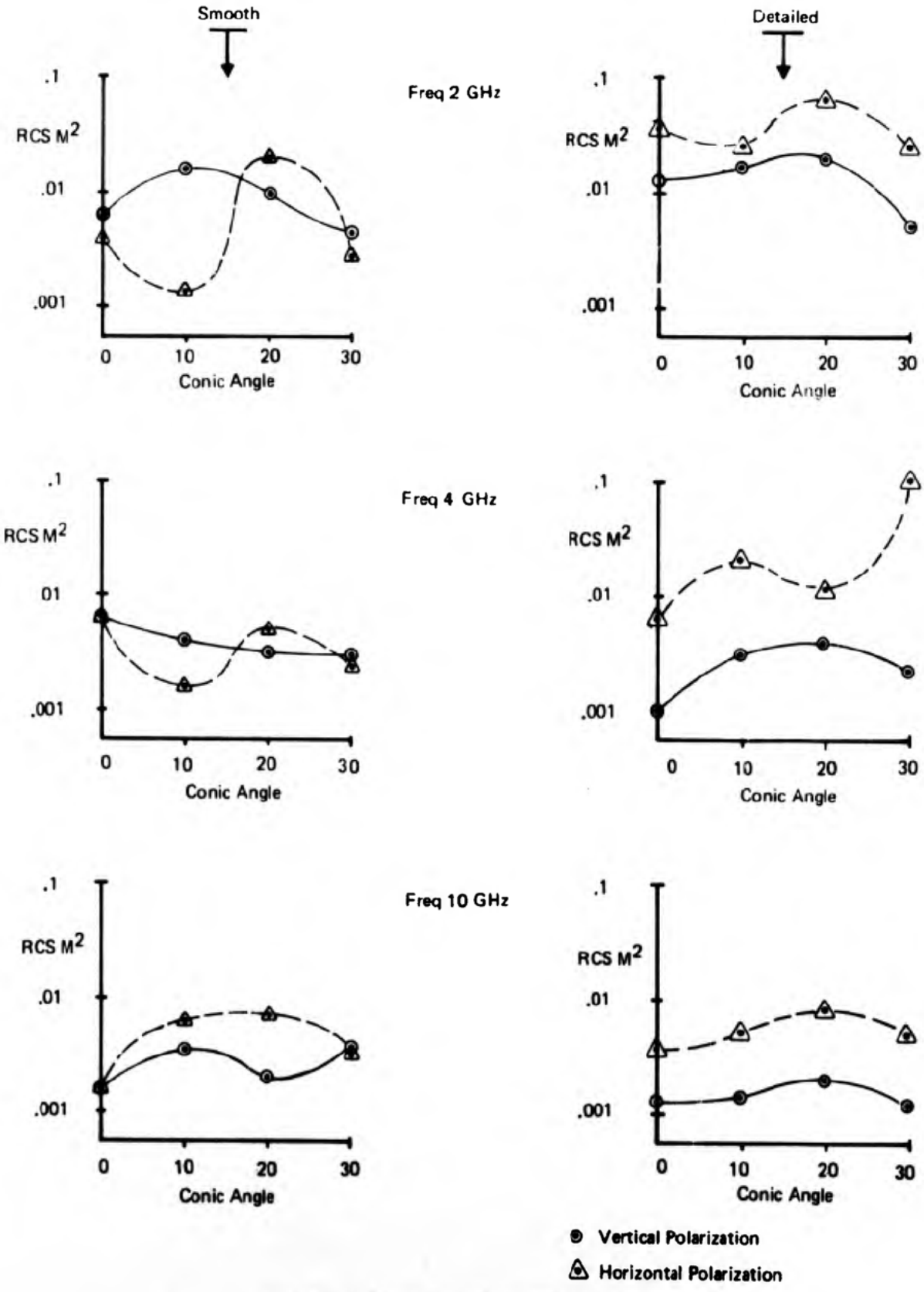

Figure 3.5: Forward Sector Median RCS (U)

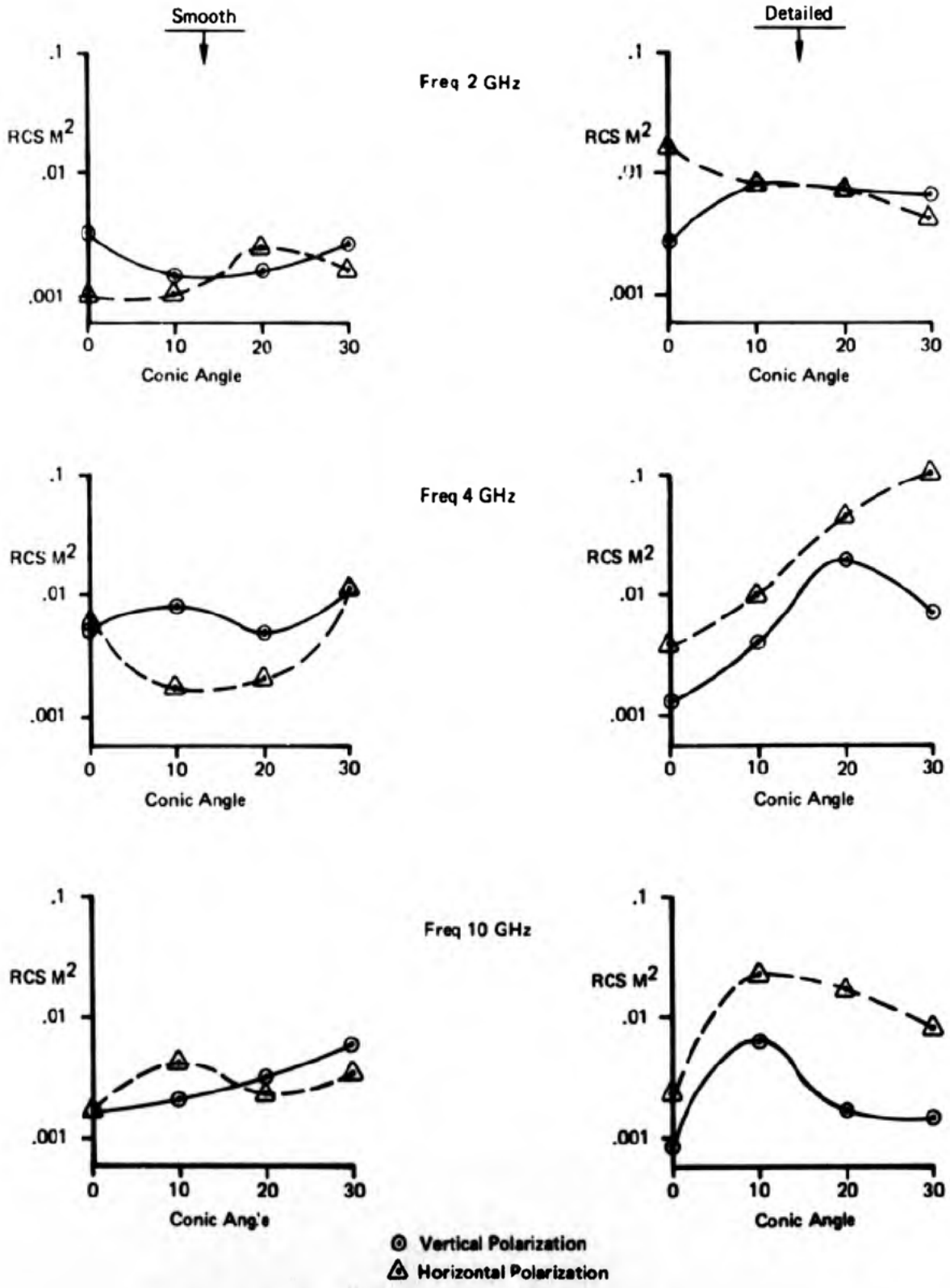

Figure 3.6: Aft Sector Median RCS (U)

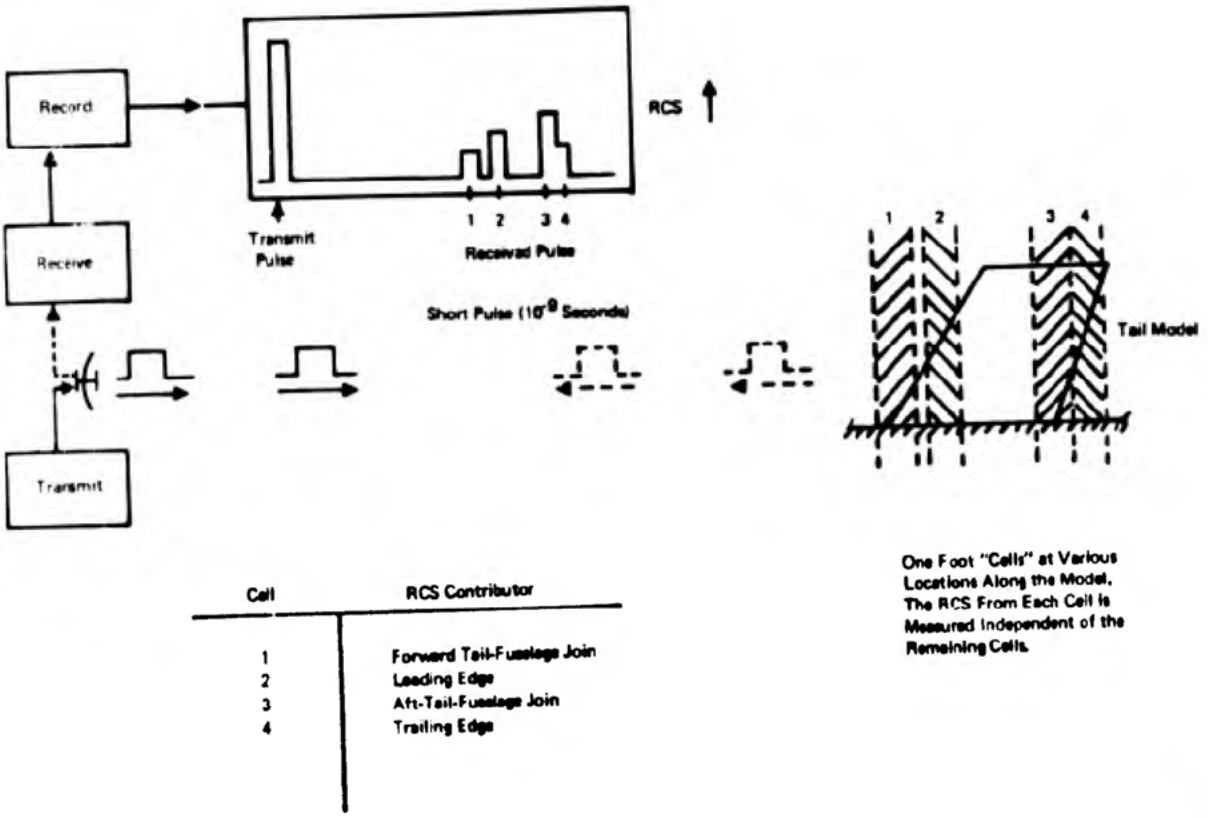

Cell	RCS Contributor
1	Forward Tail-Fuselage Join
2	Leading Edge
3	Aft-Tail-Fuselage Join
4	Trailing Edge

Figure 3.7: Short Pulse Diagnostic Concept (U)

fairing which disperses the travelling waves prior to their being reflected by the trailing edge. As a result of these findings it was decided to remove the rudder actuator fairing for the remainder of the tests for three reasons: 1) the fairing was not a significant RCS contributor, 2) the aerodynamic shape of this type of fairing would usually result in it having a low RCS, and 3) there are numerous control surfaces which would not require an actuator fairing particularly if the object had sufficient volume to install the actuator beneath the surface. The design of a control surface for low RCS must consider actuator fairings, if present, but they are not felt to be germane to low RCS design.

(C) The rudder position on the "detailed" model was varied in yaw angle from 0° to 15° in five degree steps and the respective RCS measured. The rudder position exhibited no substantial influence on the RCS. This is to be expected as most of the energy is reflected at the hinge area. If the hinge area is covered with a metallic fairing the rudder position may have more effect on the RCS. However from an aircraft operational standpoint, the rudder (or other control surfaces) will be at a near-zero degree position for the majority of the time. Maneuvers at high speed will require only small changes in the control surface position. Therefore, the rudder position was maintained at zero degrees for the remainder of the tests as this is most representative of in-flight conditions.

(C) The data on the two models revealed a large "lobe" in the RCS pattern at about 55° from nose-on for the 10° and 20° conic angles. This lobe was predominately observed at horizontal polarization which would indicate a travelling wave contribution. The two, simple, one-third scale models shown in Figure 3.8 were constructed to examine this and other RCS characteristics of the tail. The size and weight of these small models allowed for them to be studied on the indoor RCS range which saves both time and money. The one model shown is cut from a flat sheet of aluminum and the second is contoured to the lines of the full-scale model. The flat-model data was taken to determine the influence of the curved surface present on the contoured model. Measurements were made at 12GHz on these models which corresponds to a full-scale frequency of 4GHz. The flat model exhibited the lobe in the RCS whereas the contoured model did not show as clearly defined a lobe. The lobe was found to be from the trailing edge of the model and could be eliminated by placing an appropriately shaped absorber along the trailing edge. The shape of the absorber was critical and covering the entire model with absorber had no effect on the shape, location or amplitude of this lobe although the remaining RCS pattern was altered. These results led to a consideration of shaped terminations for the tail which were subsequently tested. These and the other tests performed on the model are discussed in Section 3.3, RCS Reduction Techniques.

(U) The absence of a well defined major lobe from the contoured model would indicate a problem with accuracy in the model. The overall dimensions of the model were accurate but the surface smoothness was not scaled. In fact, the one-third scale model surface

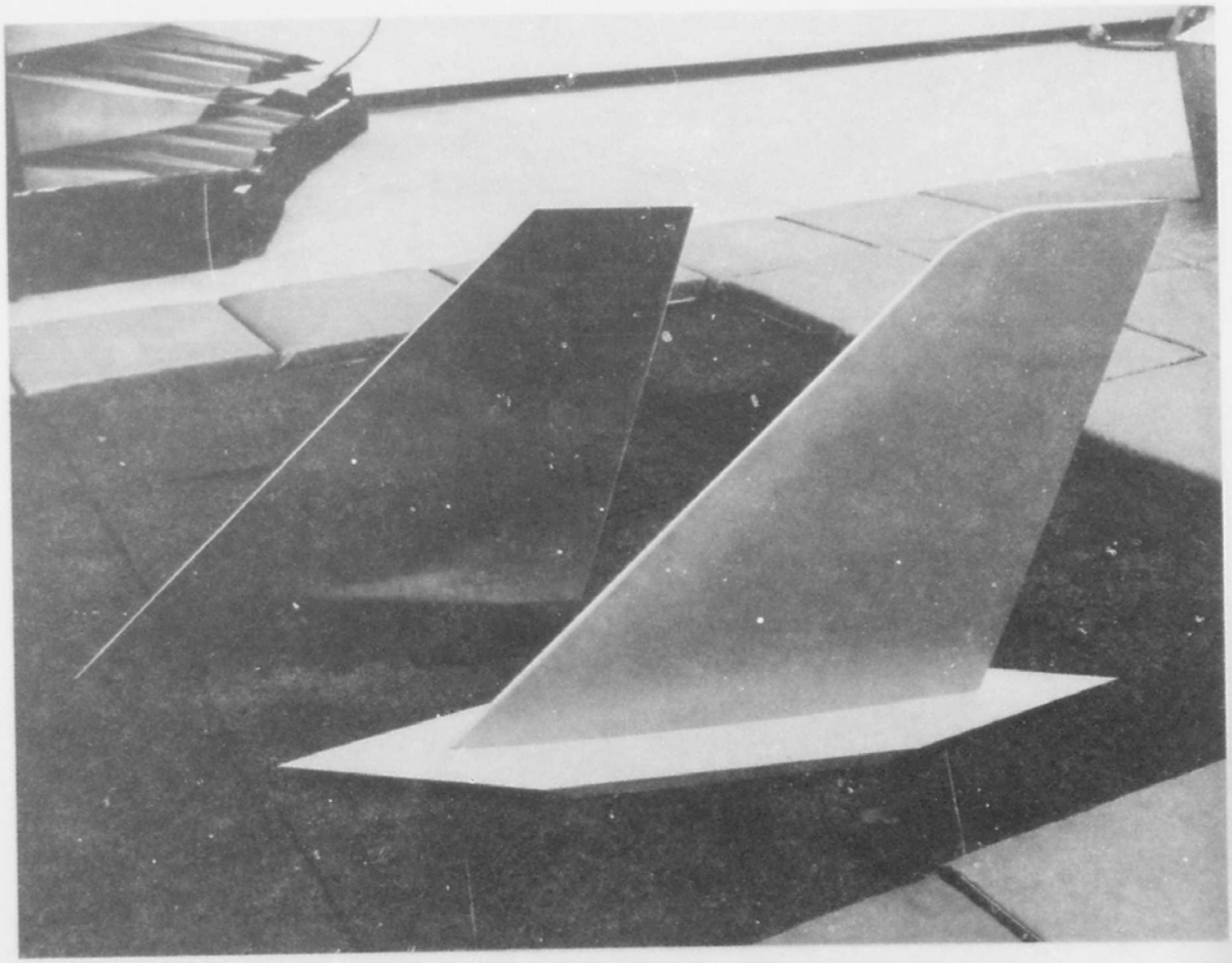

Figure 3.8: 1/3-Scale Tail Models (U)

smoothness was about equal to that of the full-scale model. Normally, this would be adequate, but travelling waves along a body are sensitive to the surface smoothness. This has been demonstrated for travelling wave antennas and will also apply for the scattering from bodies.

(U) The travelling wave RCS contribution is a predominant part of the total RCS for the tail. Therefore, it was decided to conduct a series of tests on some simple models to develop a better understanding of the scattering characteristics of the travelling waves. A series of flat rectangular plates were cut from 1/8 inch aluminum sheet stock and the edges milled to a 60° bevel. These models were all 24" wide and were 1, 2, 3, 4, 5, 6, 8, 10, 12 and 24 inches long. The models are shown in Figure 3.9. A series of measurements were made on these models at 12 GHz to determine the influence of plate size and shape on the travelling wave RCS. The magnitude, angular location and spatial distribution (beamwidth, null position) of the first travelling wave lobe was measured. The coordinate system for the plate models is shown in Figure 3.10.

(U) This portion of the program revealed several facts which bear on the RCS due to travelling waves.

1) There is no substantial dependence in the amplitude of the RCS on the length (L) but there is a length dependence as far as the location of the lobe maximum.

2) The RCS is approximately proportional to the width of the body in wavelengths.

3) The half power beam width of the travelling wave lobe in the $\emptyset$ plane (see Figure 3.10) is approximately .175 λ/W (degrees) and the first null is approximately $\sin^{-1}$ .35 λ/W (degrees) from $\emptyset = 0°$.

(U) This last result suggests that the travelling waves propagate with a velocity less than that in free space. The travelling wave is scattered by the terminating edge of the plate with a $\emptyset$ dependence that would correspond to a wire whose length is on the order of twice the width of the plate, (the travelling wave lobe has a half-power width of 17.5 λ/W whereas a wire would have a 25 λ/W half power width in the $\emptyset$ plane). These results are drawn from the data shown in Figures 3.11, 3.12, 3.13 which was taken from the measurements on the flat plate models. An exhaustive study would be required to precisely establish the relationship between RCS and plate geometry. This portion of the study provides a preliminary insight into the behavior of travelling waves along an airfoil shaped body. Further studies should be made to determine the following effects on travelling waves:

1) The influence of the radius of curvature and surface roughness

2) The reflection coefficients for various shaped terminations and different material boundaries

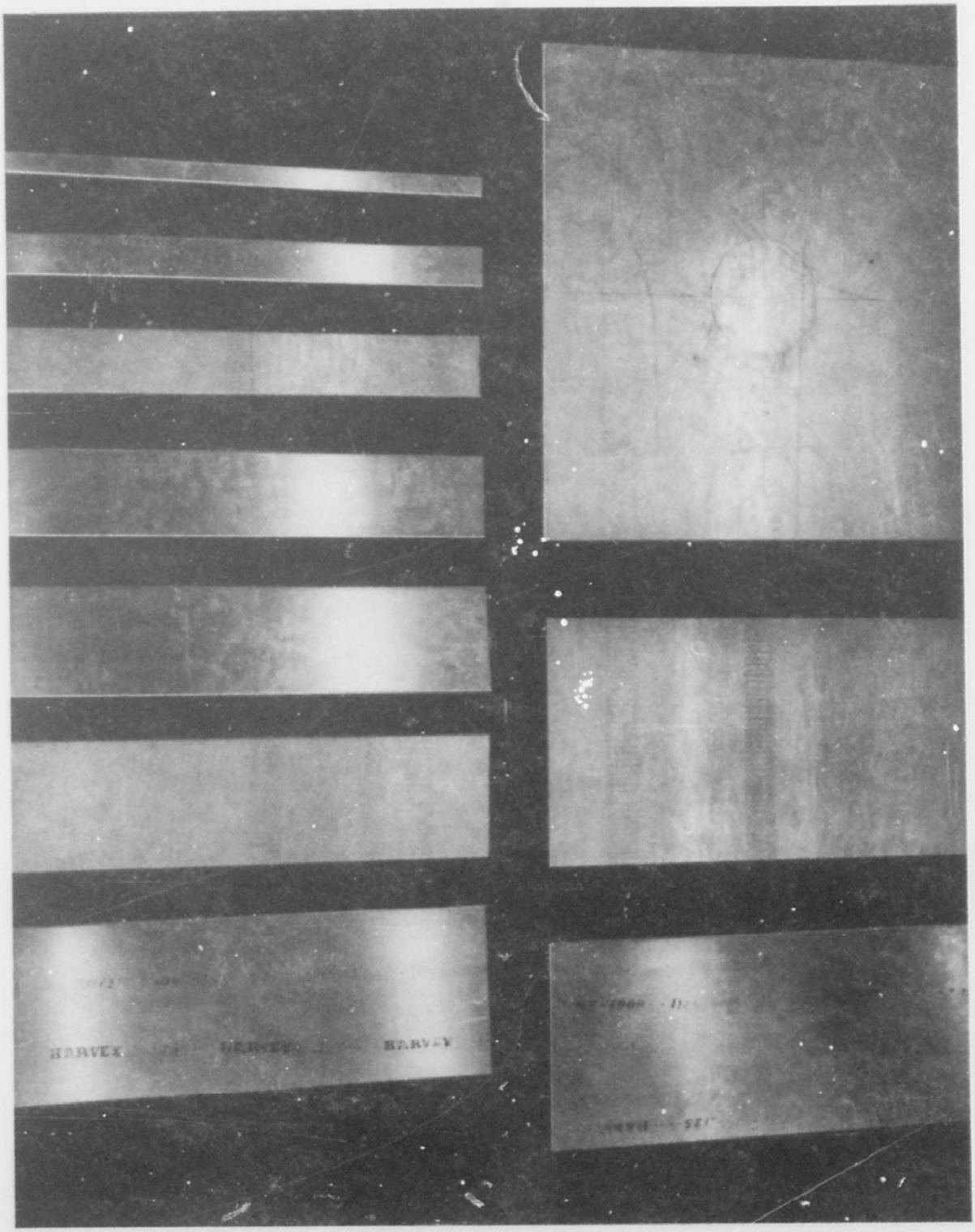

Figure 3.9: Flat Plate Test Models (U)

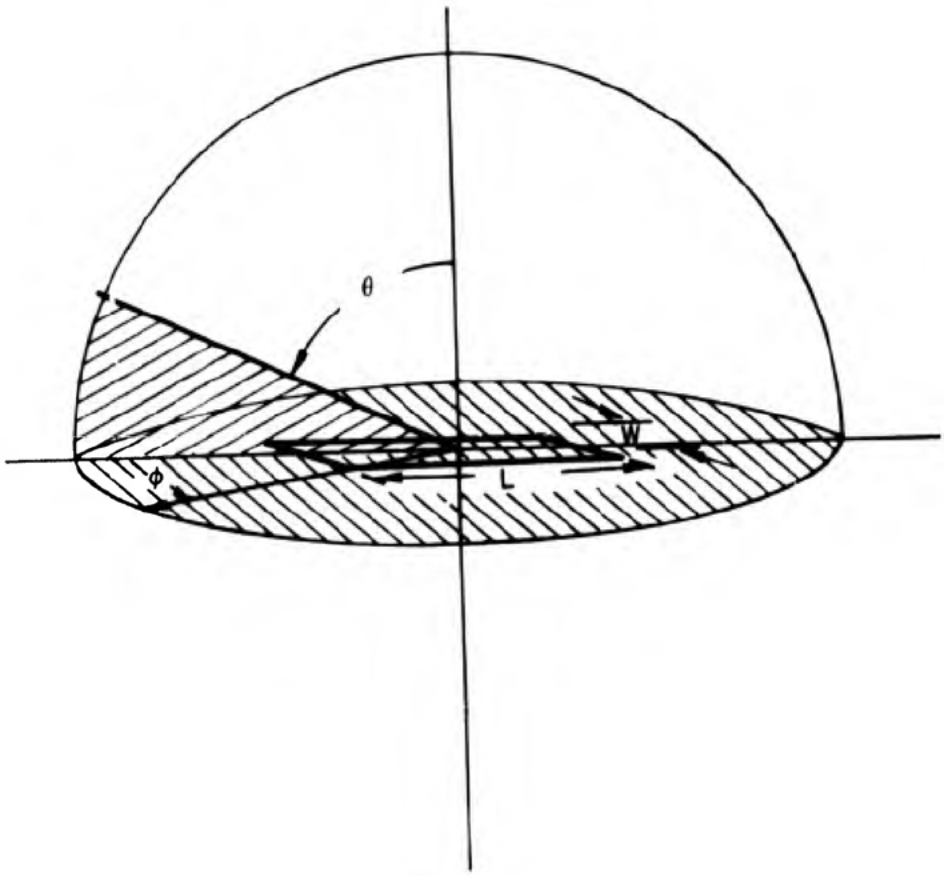

Figure 3-10: Flat Plate Coordinate System (U)

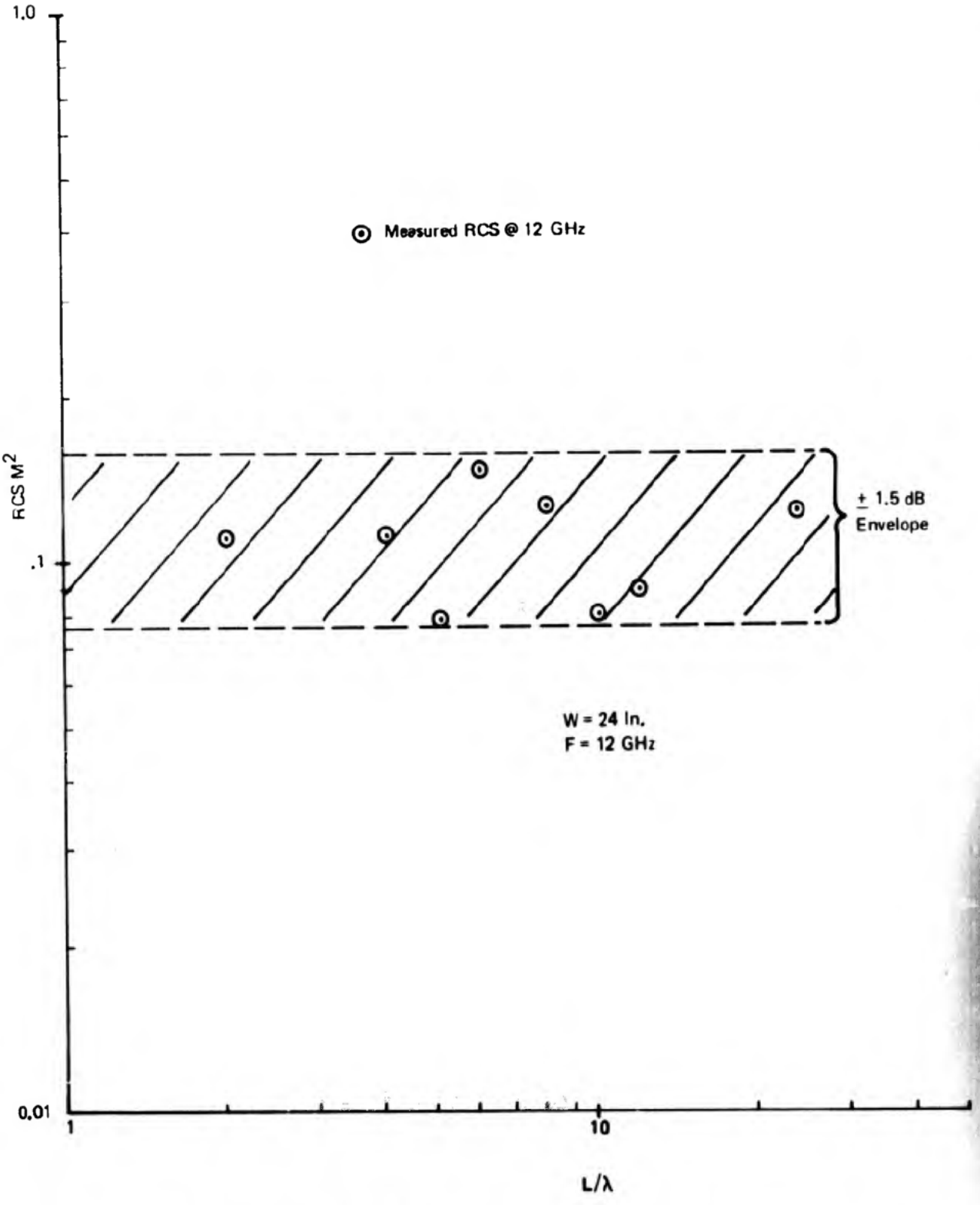

Figure 3.11: Peak Travelling Wave – RCS Versus Plate Length (U)

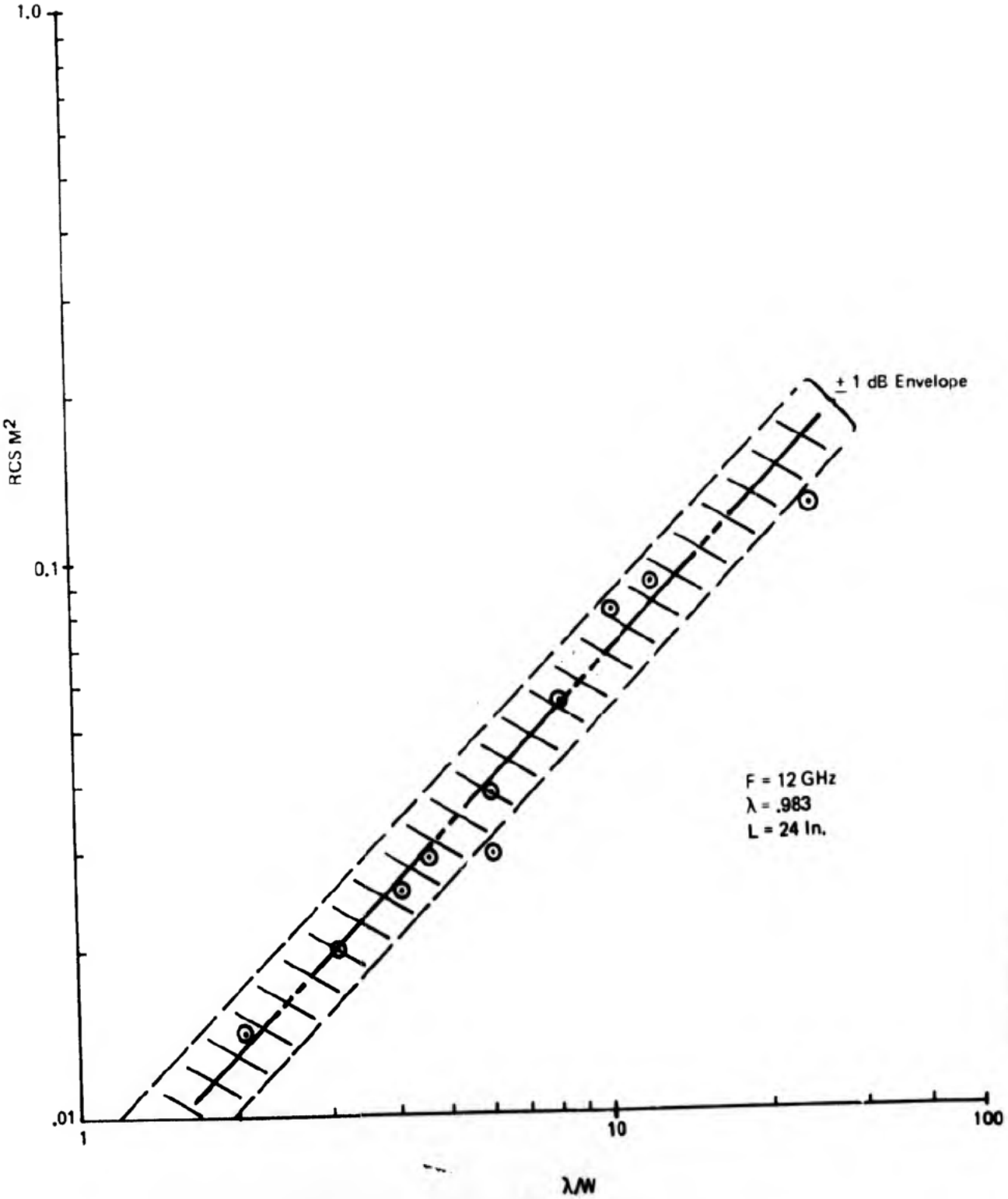

Figure 3.12: Peak Travelling Wave RCS Versus Plate Width (U)

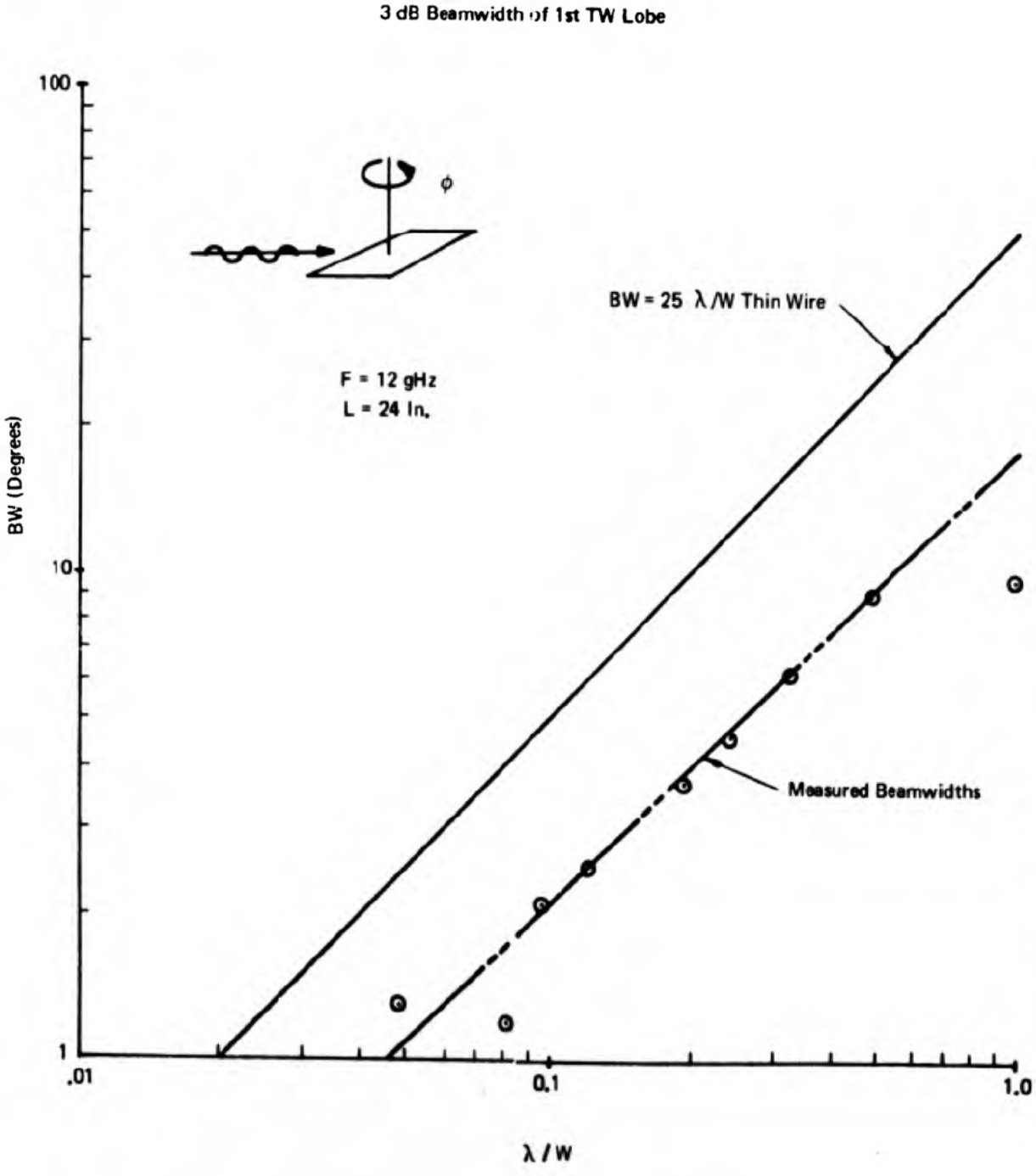

Figure 3.13: Travelling Wave Half-Power Beamwidth Versus Width (U)

3) The influence of the leading edge on the launching of these waves.

(U) These questions have been previously studied for certain bodies and some intuitive and semi-analytical results obtained. The radius of curvature is known to influence the propagation, reflection and launching of travelling waves. Surface and material discontinuties will establish a reflection point. Also, the travelling waves appear to reflect in a specular manner from a termination.

(U) Inasmuch as travelling waves appear to be predominate only for near planar surfaces, a means of calculating the travelling wave RCS for a flat plate geometry would be useful in estimating the travelling wave RCS for a control surface. A review of published work in this area did not reveal any expressions which could reasonably predict the travelling wave contribution for flat plates. The work of Ross[1] using the geometrical theory of diffraction for flat plates shows good agreement with theory at all but near-grazing incidence. The work of Peters[2,3,4,5] has shown good agreement with experimental data for the travelling wave RCS from thin wires, but does not agree with the measured data for flat plates. Therefore it was decided to incorporate the results of the flat-plate model measurements into an expression which describes the travelling wave RCS.

(U) The expression developed by Peters was used as a basis for predicting the angular location of the travelling wave and the magnitude of the travelling wave was determined empirically from the data taken during this study. The Peters expression for the RCS of a thin wire (σ), assuming a wire long in wavelengths and a phase velocity equal to that of free space is:

$$\sigma = \frac{\gamma^2 \lambda^2}{\pi} \left[\frac{\cot^2(\pi - \theta/2) \sin^2[2\pi L/\lambda \sin^2(\pi - \theta/2)]}{\ln(4\pi L/\lambda) - 0.4228} \right]^2$$

where:

γ = reflection coefficient at the terminating edge.

λ = wavelength

L = length

(U) The extensive flat plate RCS data taken during this program was then used as a basis for determining the magnitude of the travelling wave RCS as a function of plate length and width. A review of published work on travelling waves has not revealed any experimental data on planar surfaces which cover the range of width and length to wavelength ratios studied during this program. This experimental data base was developed as it was the most effective means of rapidly determining the behaviour of travelling waves on planar surfaces.

(U) The $\sin^2(\ 2\pi L/\lambda \ \mathrm{SIN}^2(\pi - \theta/2) \ )$ dependance of the above expression was combined with the observed dependence of the travelling wave RCS (σ_{TW}) on plate width as follows:

$$\sigma_{TW} = 10 W \lambda \gamma^2 \cos^{2n}[2(\theta + \theta_n)] \ \mathrm{SIN}^2[(2\pi L/\lambda) \ \mathrm{SIN}^2(\pi - \theta/2)]$$

where:

W = plate width

n = 1,2,3,4. . . . (n=4 provided a good fit to the measured data)

$\theta_n = 49.35\sqrt{\lambda/L}$

This expression for the RCS from travelling waves was then combined with the physical optics expression commonly used for near-normal incidence RCS calculation as follows:

$$\sigma = \left[\frac{4\pi L^2 W^2 \cos^2\theta \ \mathrm{SIN}^2(2\pi L/\lambda \ \mathrm{SIN}\theta)}{\lambda^2[(2\pi L/\lambda) \ \mathrm{SIN}\theta]^2}\right] + \sigma_{TW}$$

(U) This in effect is the arithmetic sum of the "specular" and travelling wave RCS returns. A more exact expression would employ a phasor sum of these returns. Assuming the travelling wave RCS originates at the trailing edge of the plate and the "specular" return is due to the diffraction at the plate edges, an expression relating the phase of the two types of returns can be developed. However, this requires that the phase velocity along the plate surface be known. Development of a more detailed expression for the plate RCS was not explored as the above expression showed good agreement with the experimental data and is sufficient for estimating the approximate level of RCS from near-planar control surfaces. This agreement is shown in Figure 3.14 for plates of 24 inch width and for lengths of 4,5,8 and 10 inches. A similar set of data is shown in Figure 3.15 for plates of a constant 24 inch lengths and for widths of 4,5,8 and 10 inches. The agreement about the travelling wave lobe peaks and in their location is good, The curves of Figure 3.16 and 3.17 show the peak RCS envelope of the calculated curves and the measured RCS peaks.

(U) The results of this analysis and the expressions developed provide for a preliminary understanding of the travelling wave RCS for a flat plate geometry. The application to a more complex surface such as the vertical tail, was also examined. A rectangular plate representation of the vertical tail was developed as shown in Figure 3.18. This geometry represents the area of the tail model. Using this simple model the RCS due to the entire tail and the rudder alone was calculated using the expression previously discussed. A comparison between the calculated RCS for the rectangular geometry and the measured RCS of the tail model indicates that the rudder alone contributes the majority of the travelling wave RCS. The travelling wave RCS calculated for the rudder alone and the measured RCS

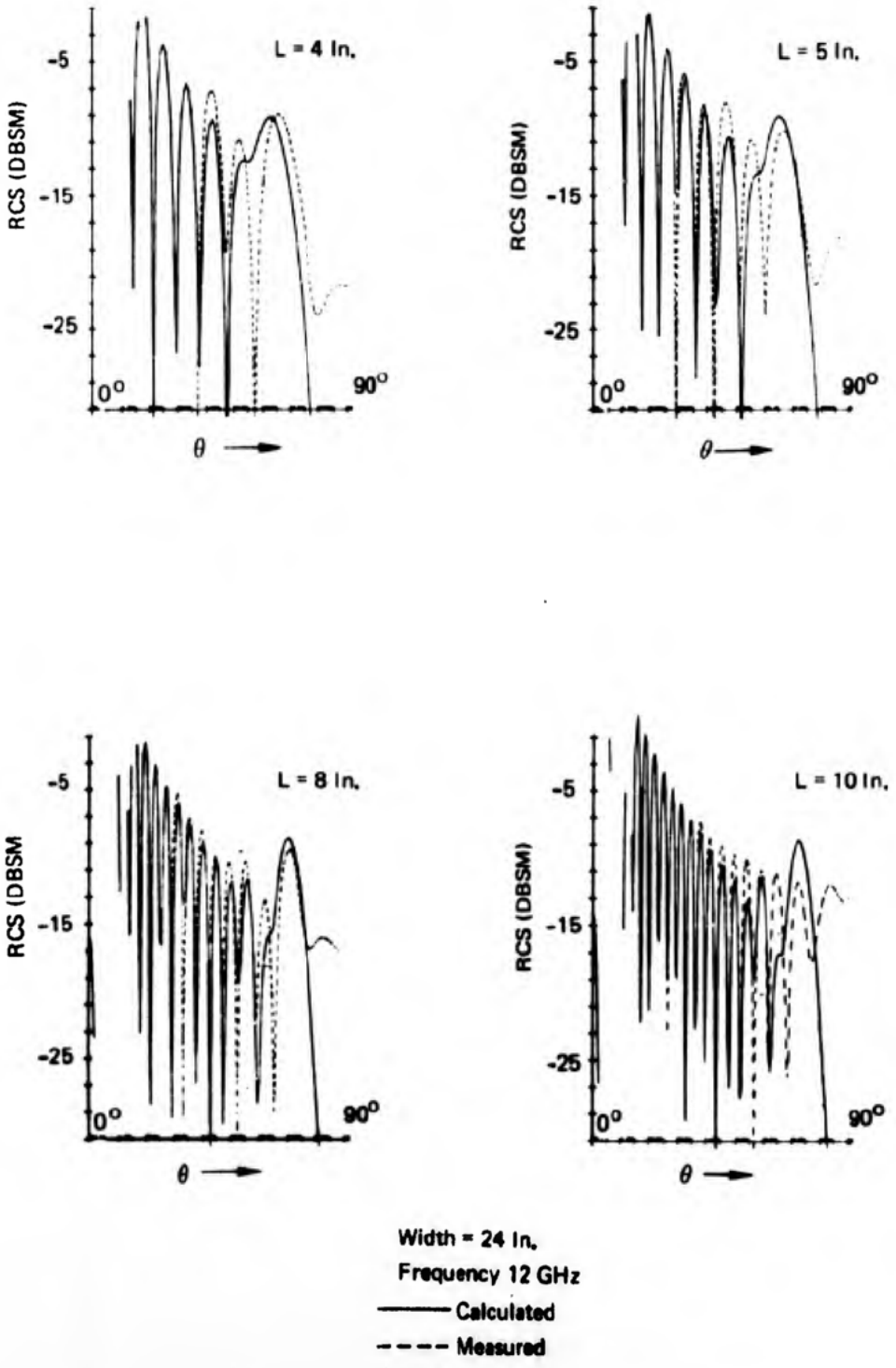

Figure 3.14: Flat Plate RCS for Various Lengths (L) (U)

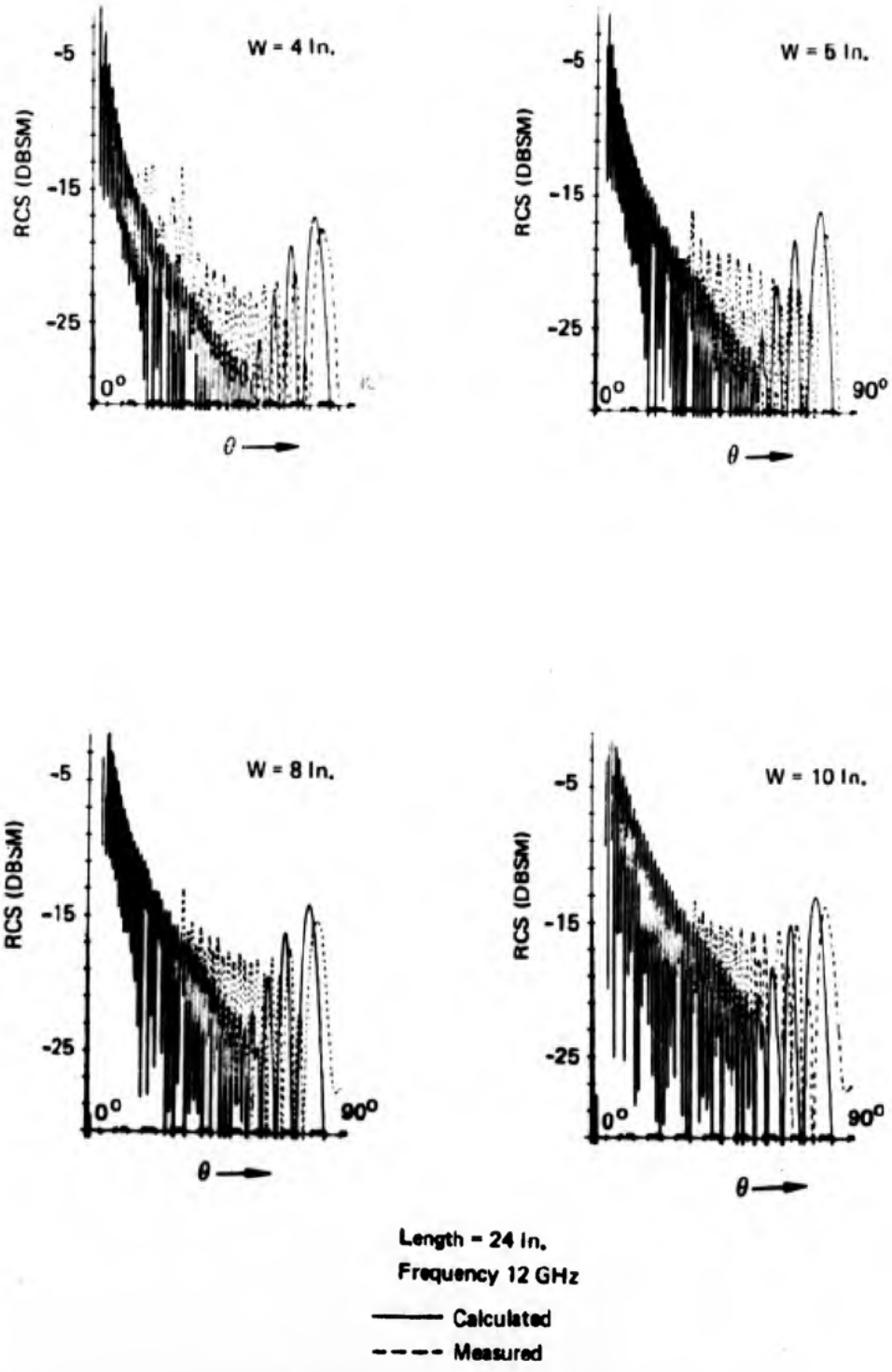

Figure 3.15: Flat Plate RCS for Various Widths (W) (U)

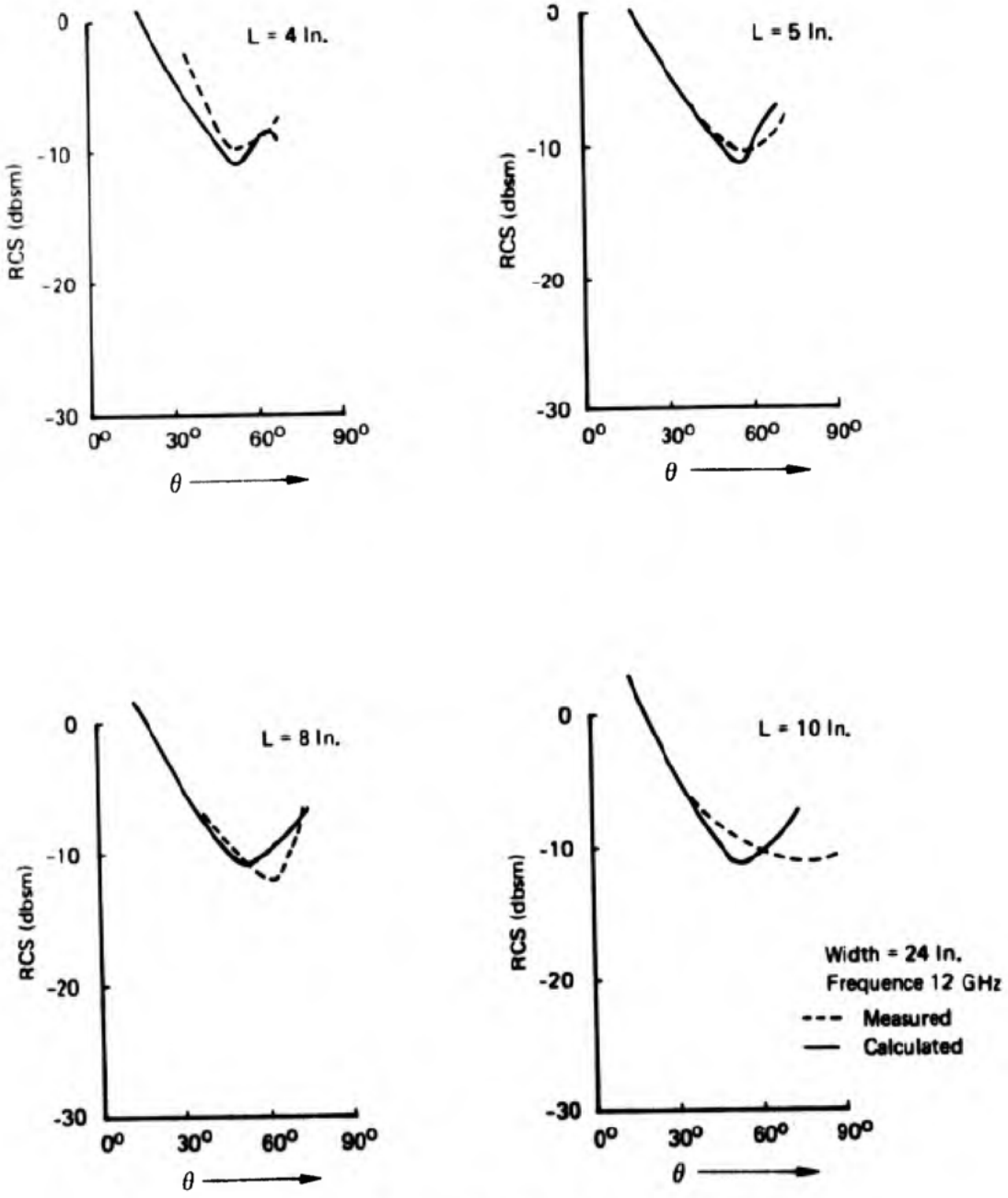

Figure 3.16: Flat Plate RCS for Various Lengths (L) (U)

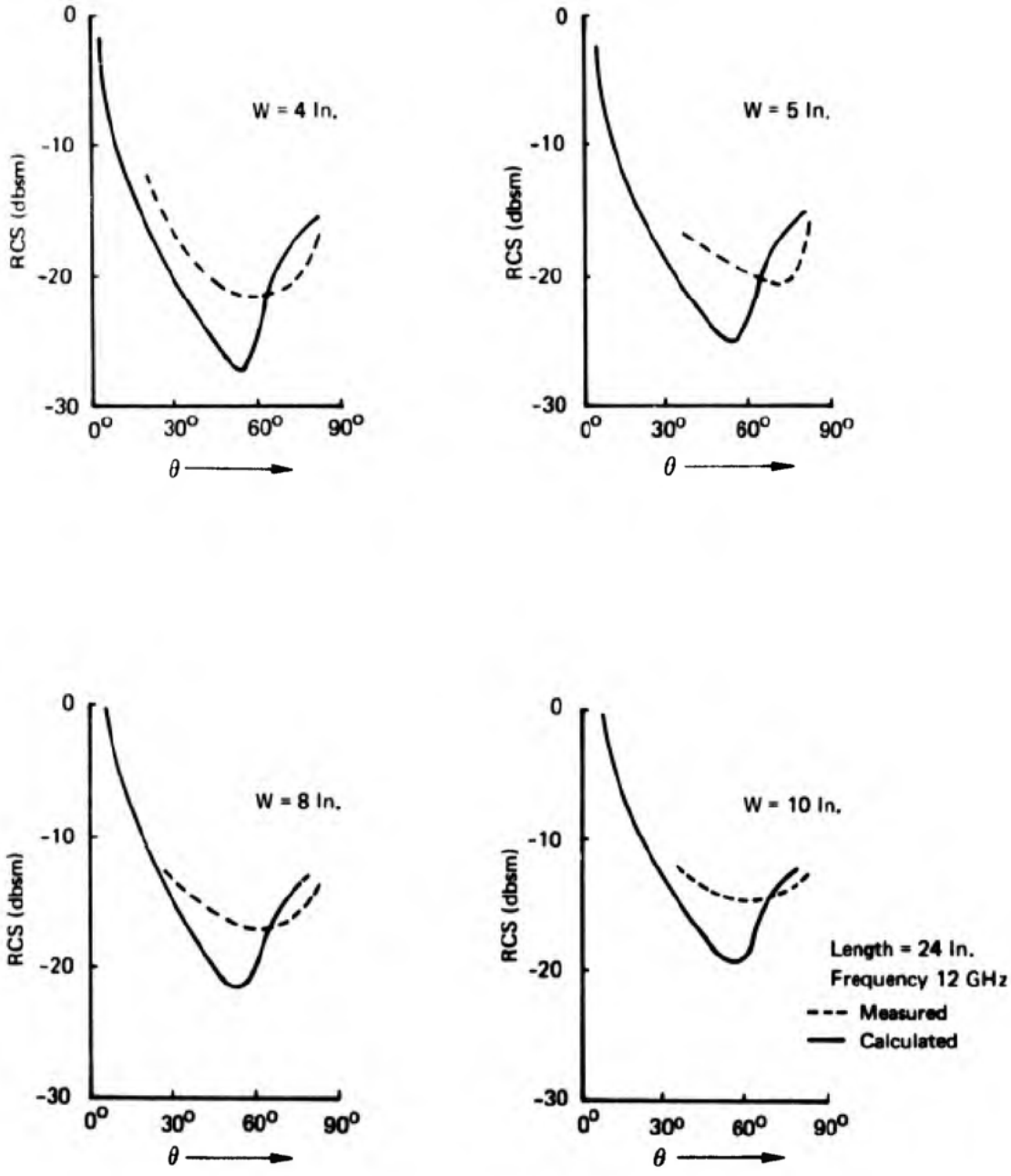

Figure 3-17: Flat Plate RCS for Various Widths (W) (U)

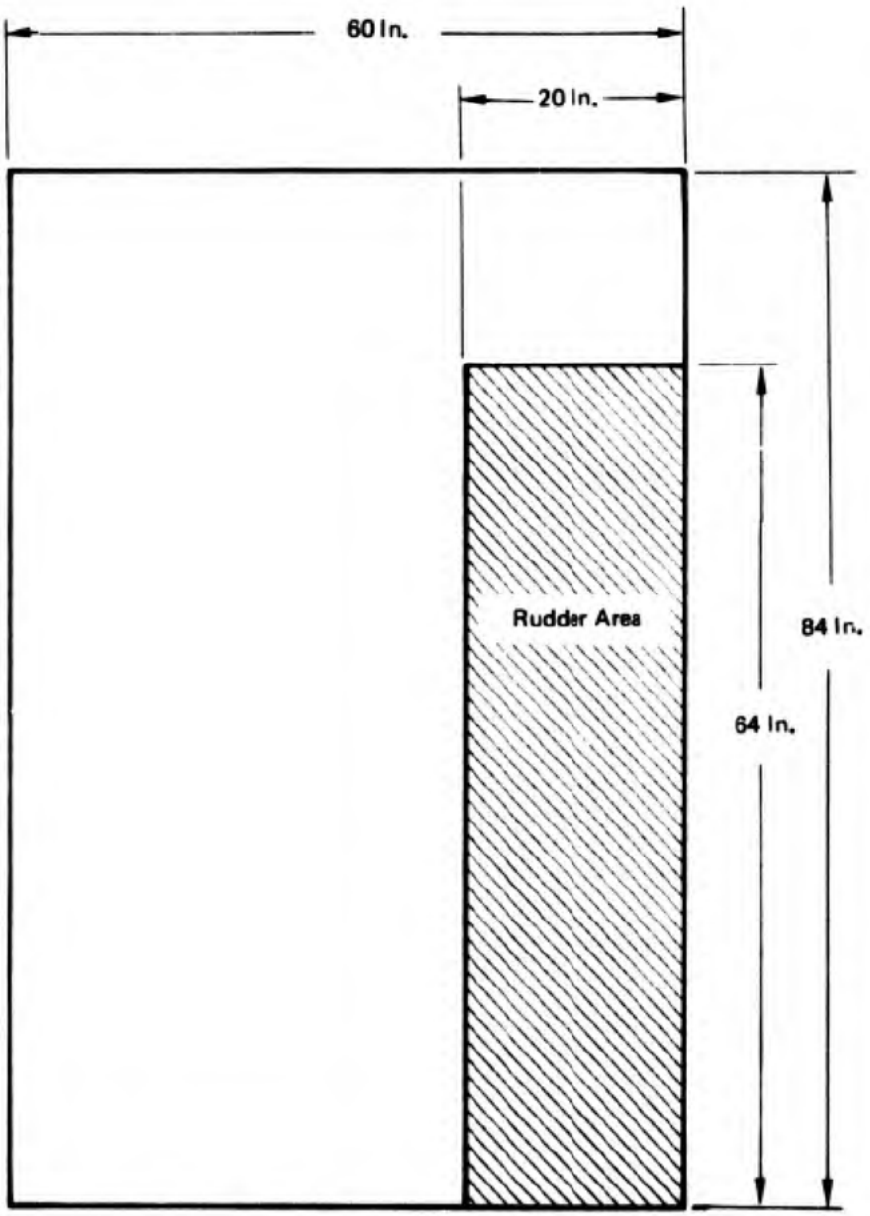

Figure 3.18: Rectangular Tail Model (U)

of the tail model is shown in Figure 3.19 at 2.0 GHz. The large lobe at about 30° in the calculated RCS and at 40°-45° in the measured show a reasonable agreement considering the simplifying assumptions made.

(U) An approximate expression to determine the extent and distribution of travelling wave backscatter has been developed during this study. This expression will assist in the analysis of the travelling wave RCS problem. A more refined and accurate expression is desirable and is a worthy candidate for future research.

3.3 RCS Reduction Techniques

(C) In general it is possible to alter the geometry and surface of a body in several ways to influence the travelling wave RCS. The length can be chosen to establish the angle for the travelling wave lobe. The width can be reduced to minimize the RCS. The shape of the termination can be altered to scatter the reflected travelling wave into non-critical sectors. Absorbers can be applied to attenuate the travelling waves and can also be shaped to minimize the reflection from the absorber edges.

(S) Several candidate methods were selected for reducing the RCS from the vertical tail. An electrically conductive fairing to cover the rudder hinge area is one obvious technique. Similarly, the fairing of all panel joins to remove these discontinuties was considered. Both of these methods are effective and have essentially no significant influence on the weight or cost of the structure.

(S) Absorber terminations for the travelling waves were also considered for application to both the leading edge and trailing edge regions. The use of a magnetic material on these regions was shown to be effective during the initial phases of the program using "lay-over" material applied to the surface. The use of structural absorber materials was an objective during this program. Therefore a suitable structural magnetic absorber material was required. Available absorbers would not suffice for this tail application and a new material had to be developed. A laminate of fiberglass using an epoxy resin matrix loaded with colloidal iron particles was judged to be a reasonable starting point for developing a suitable material. A series of specimens for both electrical and strength tests were constructed using various amounts of magnetic material. A commercially available iron-loaded, resin system (Emerson and Cummings CR-124) was used as the impregnating resin for fabricating these specimens. The CR-124 was mixed with a non-loaded epoxy resin in ratios of 0, 25, 50, 75 and 100 percent CR-124 (by volume). This resin mix was then used as a binding matrix for a laminate using five layers of fiberglass cloth. These samples were tested for flexure, interlaminar shear and tensile strength. The processing of these samples is not developed and the quality of the parts was not as good as could be expected with more experience. The structural tests indicate the feasibility of using this type of material and it

Frequency 2 GHz

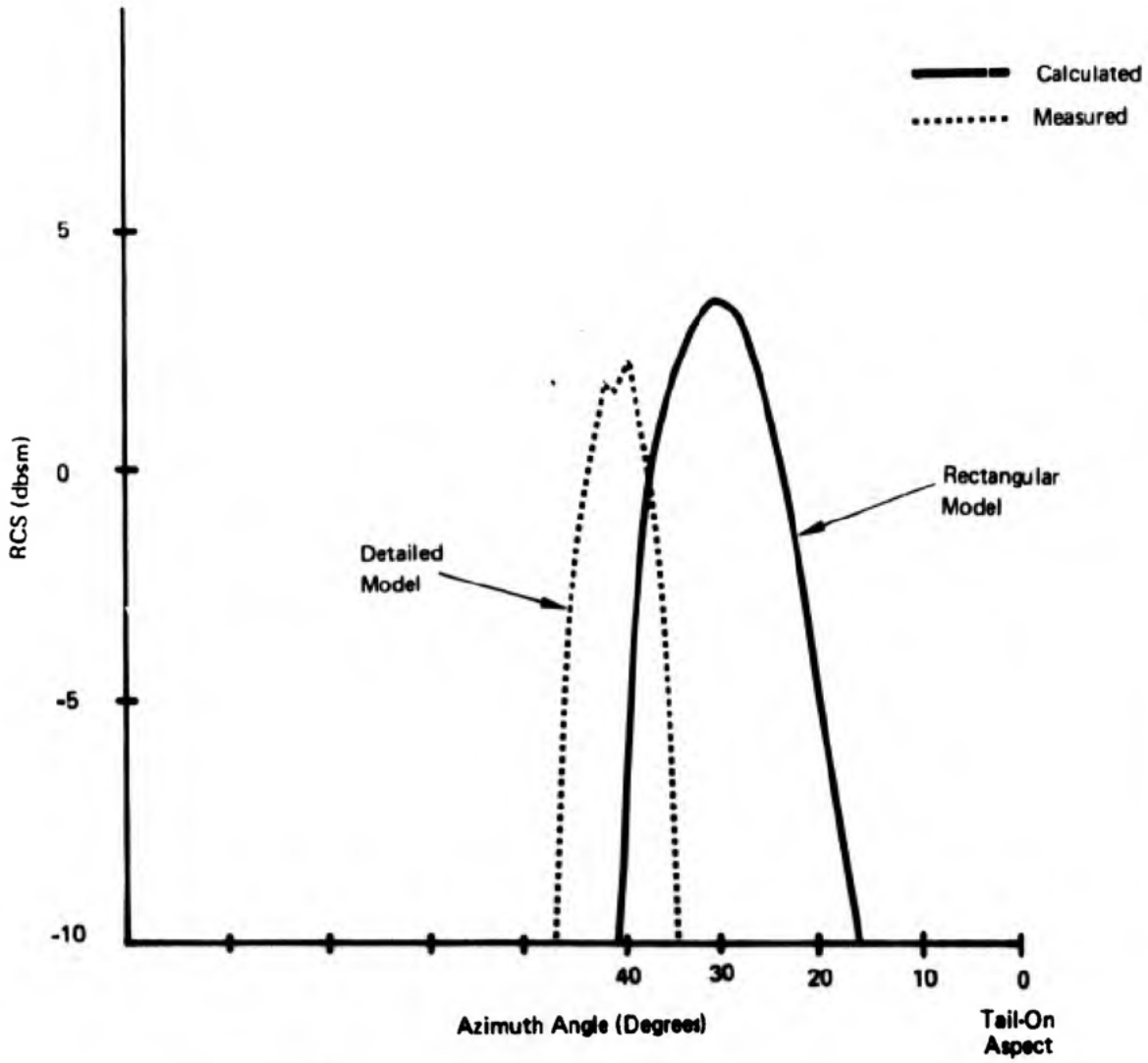

Figure 3.19: Traveling Wave RCS (U)

(S) is expected that with improved processing the strength could be significantly increased. The structural test data is summarized in Figures 3.20, 3.21 and 3.22. The 25% loaded sample was not of sufficient quality to test and therefore this point is excluded from the curves. In general the material apparently decreases in flexure strength as the loaded resin is added. However, the failure mode for these tests was determined to be in interlaminar shear and therefore the data is not necessarily an accurate measure of the flexure strength. The overall strength of the loaded resin laminates is sufficient for use in the design of a vertical tail structure, although the amount of backup structure required is not presently defined.

(U) Experimentation with the processing of the materials resulted in some improved specimens which were subjected to electrical tests to evaluate their effectiveness of attenuating travelling waves. These samples were 6"X12" and were fastened to one side of a 6"X12" metal plate. The normal incidence (specular) and travelling wave RCS was measured from both sides of the plate (metal and absorber) and the attenuation determined. This method is accurate for measuring the travelling wave attenuation for levels to about -10db. Beyond this point the travelling wave cannot be distinguished clearly from the edge return from the plate.

(U) The attenuation for these samples is shown in Figure 3.23 as a function of frequency. In addition a sample of pure CR-124 with no fiberglass incorporated was tested. The measurements show a growth in travelling wave absorption with increased loading up to a point equalling the pure CR-124. Furthermore, a significant normal incidence absorption is achieved particularly at the lower frequencies. It is likely that the thickness of the material can be altered to improve the normal incidence absorption. This was not done as data was not available on the complex permittivity (ε) and permeability (μ) of the material. These data are required to design for normal incidence absorption.

(U) The weight per square foot of these samples are shown in Figure 3.24. The 100% CR-124 laminate weighs about 2.3 lb/ft^2 which is a factor of about six greater than the unloaded specimen (.4 lbs/ft^2). The specimen thickness increases with loading as the number of plies of fiberglass were held constant to maintain the strength.

(S) The preliminary tests substantiate the feasibility of incorporating these materials into an aircraft structure. Therefore, a leading edge fairing, rudder and the trailing edge of the tail above the rudder were constructed from a 100% CR-124 loaded laminate for testing. These parts are shown as installed on the model in Figure 3.25.

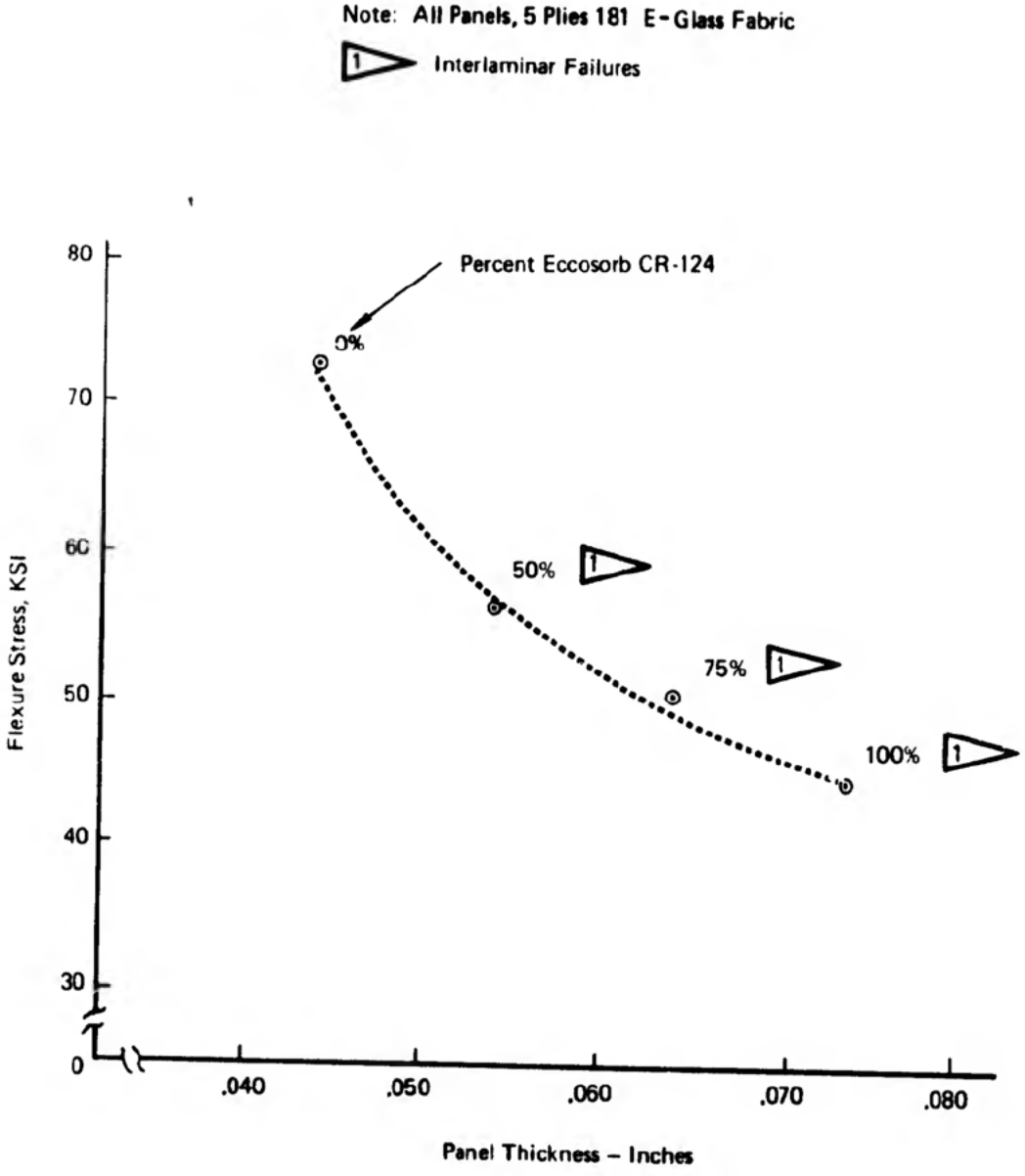

Figure 3.20: Flexure Strength Data (U)

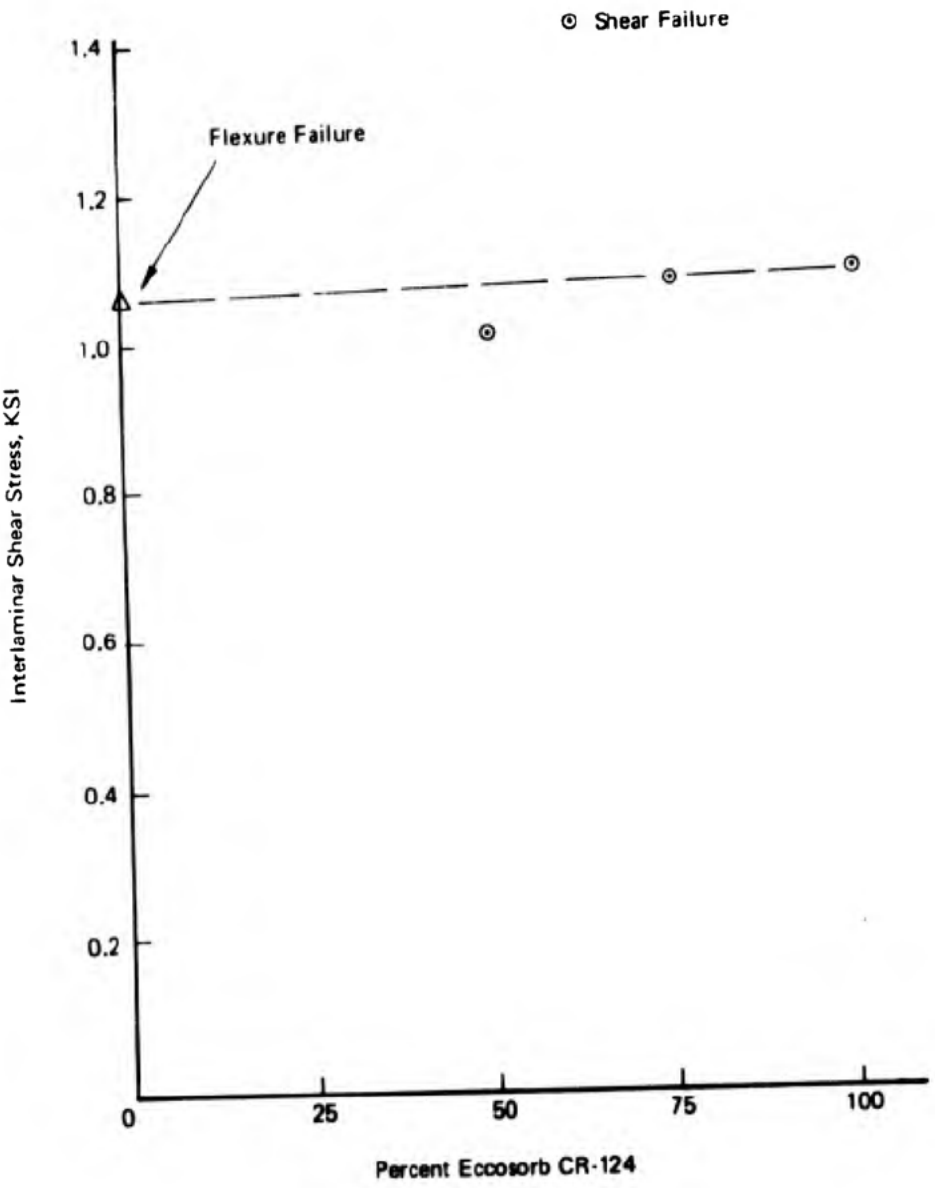

Figure 3-21: Interlaminar Shear Strength Data (U)

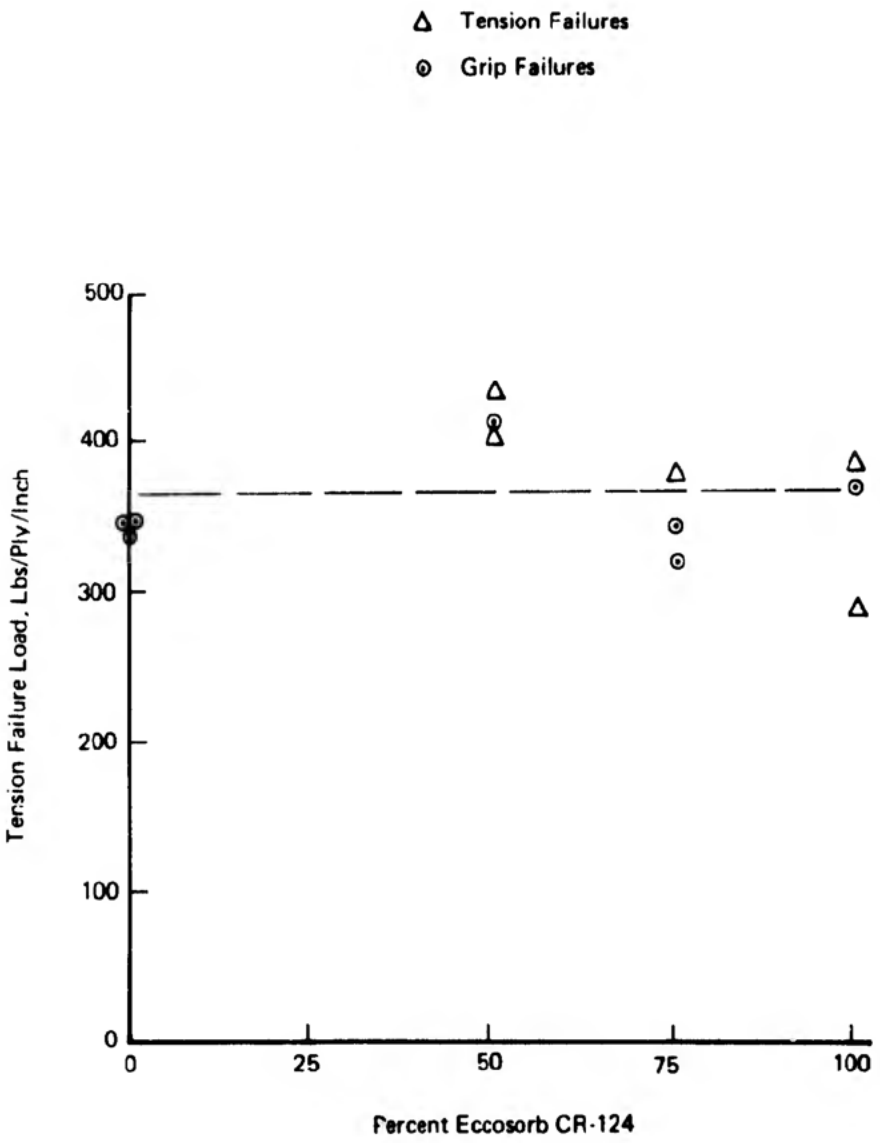

Figure 3.22: Tensile Strength Data (U)

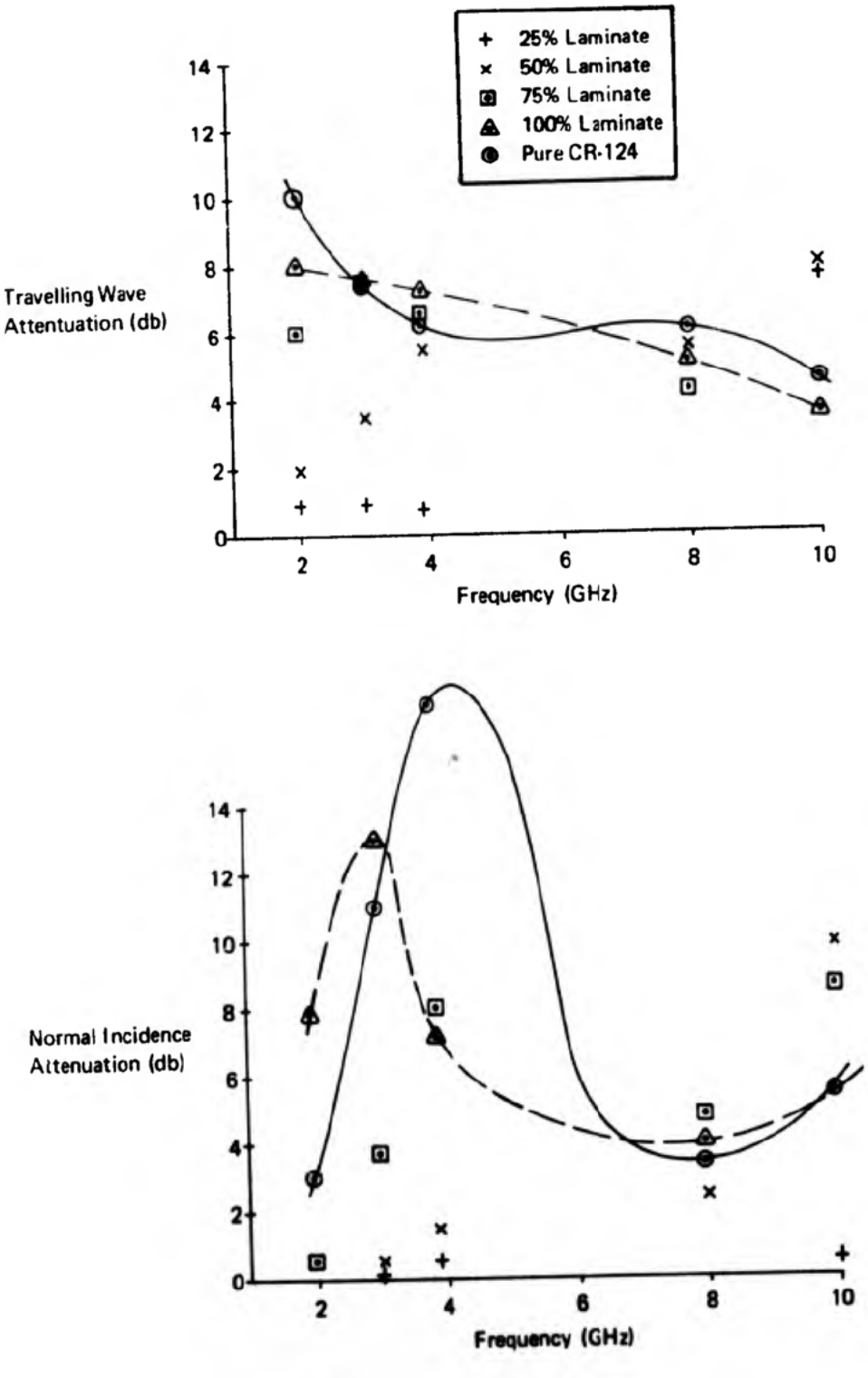

Figure 3-23: Magnetic Absorber Performance (U)

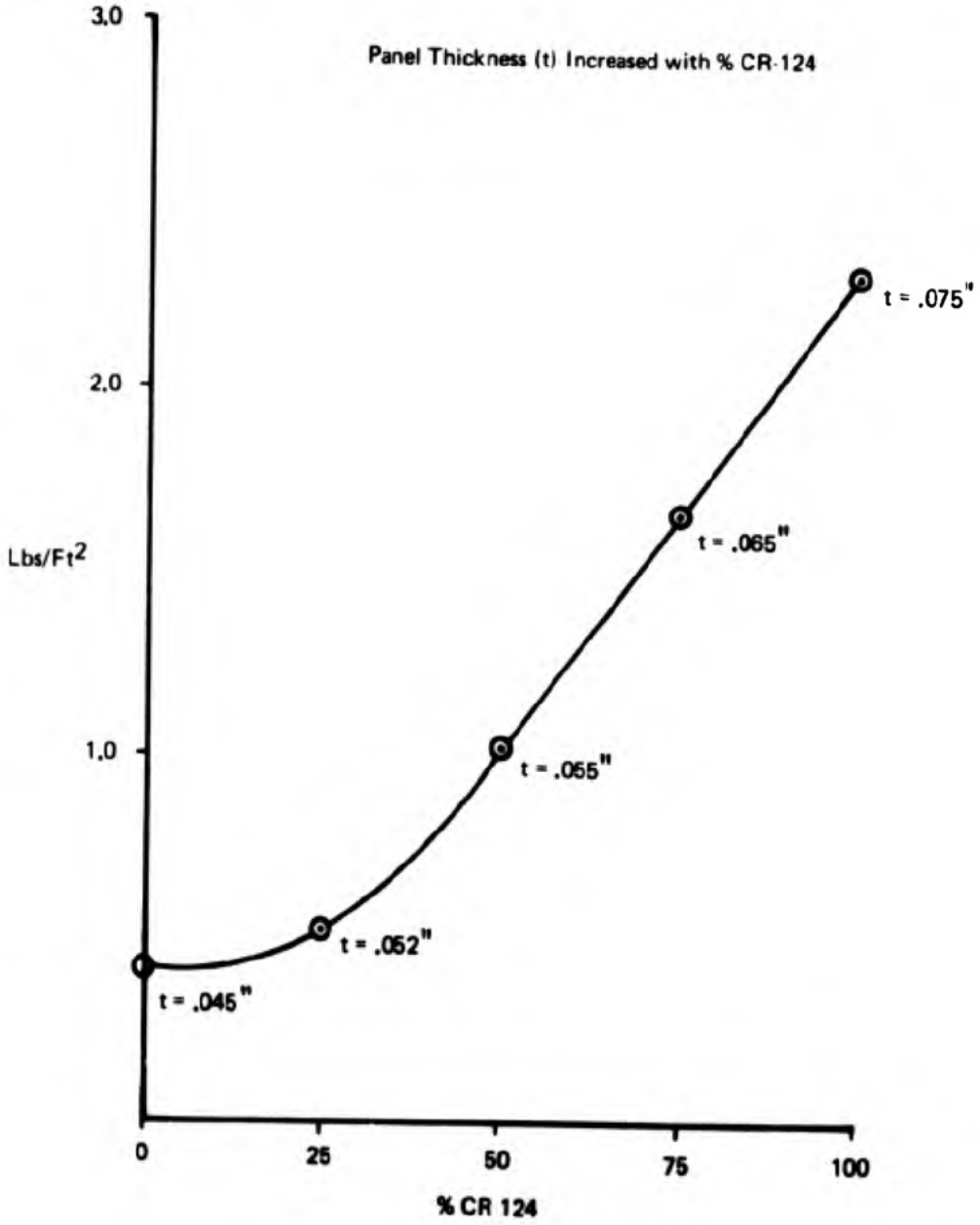

Figure 3-24: CR-124 Laminate Weight (U)

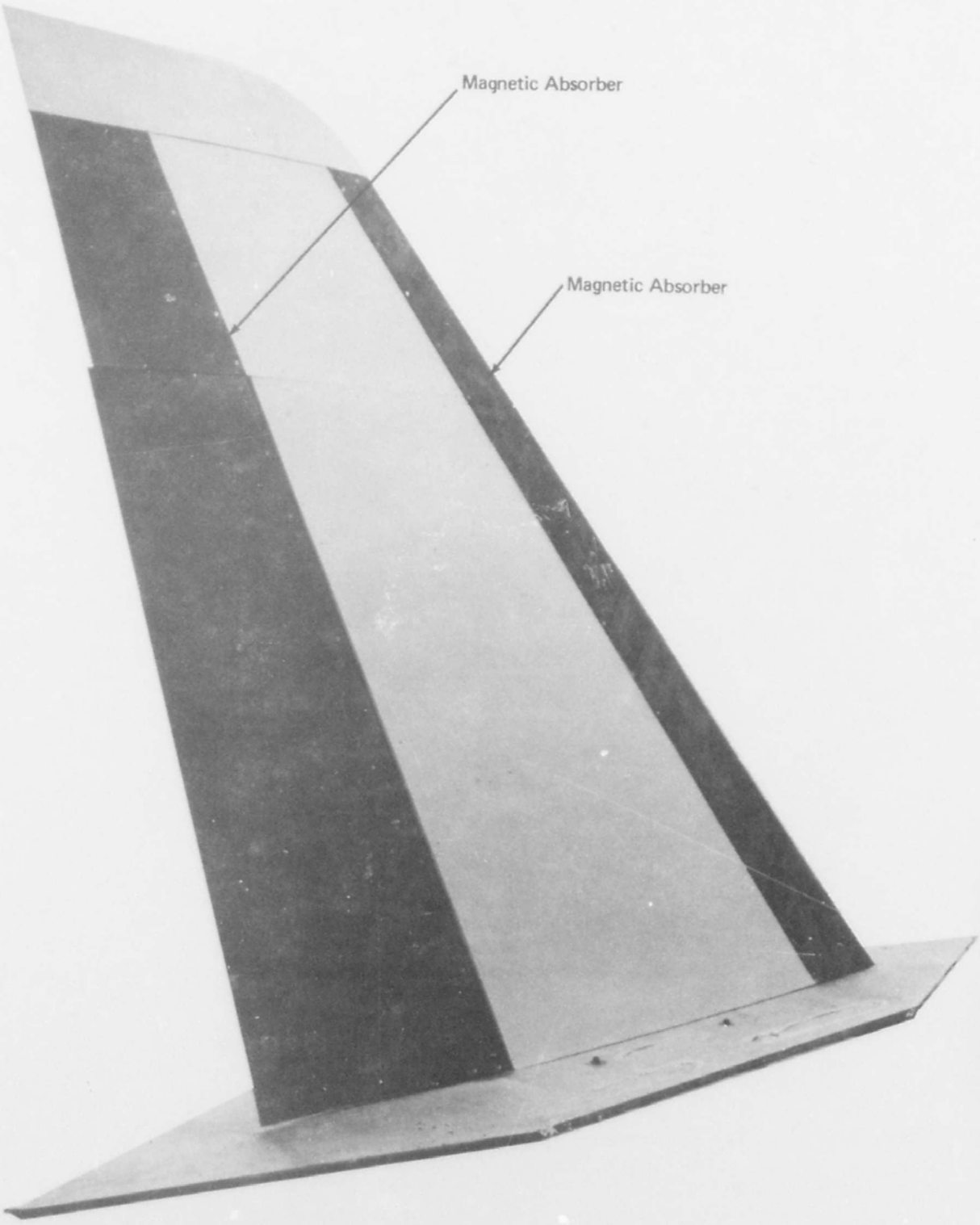

Figure 3.25: Magnetic Ram Installation (U)

(S) The reduction of the broadside sector RCS was also a program objective. One technique studied to accomplish this was to design a transmissive structure for the tail side surfaces. This structure would be similar to a radome in that the majority of the radar energy would pass through the structure. An "A" sandwich (a radome terminology) consisting of a honeycomb core sandwiched between two electrically thin fiberglass skins was selected as the most promising technique. The strength required for this sandwich restricted the minimum skin thickness to between .020" and .030". Similarly, the minimum density honeycomb that is allowable structurally was about 5 lbs./ft.^{3}. The maximum reflection coefficient for a low density (5 lbs/ft^3) honeycomb covered with either .020" or .030" epoxy-fiberglass skins is shown in Figure 3.26 and 3.27 at normal incidence (0°) and at 30° from normal incidence. It was assumed that the honeycomb thickness would vary from one inch to four inches in thickness on the actual tail due to volume constraints. The curves represent the worse case reflection and the values are much lower at some frequencies for certain thicknesses of material. The reflected energy shown is comparable to that from a broadband, structural, specular absorber material. The transmissive panels are much lighter and less expensive than most absorbers. The RCS of the interior surfaces would have to be allowed for in a design using transmissive structure. The various spars, struts and structural members would have to be appropriately shaped or treated to minimize the RCS. A series of thin fiberglass panels were built to cover the vertical tail model as shown in Figure 3.28. These panels electrically represent the honeycomb sandwich panels with the .020 inch skins. This panels were then evaluated by measurements on the RCS range as described later.

(S) In addition a set of side panels (as shown in Figure 3.29) were constructed from a structural, circuit-analog absorber. This specular absorber material is designed to provide nominally 13 db of absorption from 2-12 GHz. The CA absorber panels were only installed over the center portion of the tail due to volume restrictions. A thinner CA absorber to fit the more confined regions on the tail would have to be used on the actual tail. The thinner CA would probably not provide sufficient absorption at the lower frequencies (below 4 GHz).

(C) A series of tapered terminations along the absorber-metal interfaces and on the trailing edge were also designed for inclusion on the model. These devices are shown in Figure 3.30. The geometry of these terminations are designed to scatter the travelling waves and reflect them into non-critical areas.

3.4 Model Test Results

(C) The RCS reduction techniques described in Section 3.3 were installed, singly and in various combinations, on the full-scale tail model. RCS measurements were made at 2, 4 and 10 GHz on these various model configurations to establish the RCS reduction achieved. The RCS for each configuration was examined in detail and a preliminary design configuration established. The RCS data has been summarized in terms of the ten degree median values at each conic

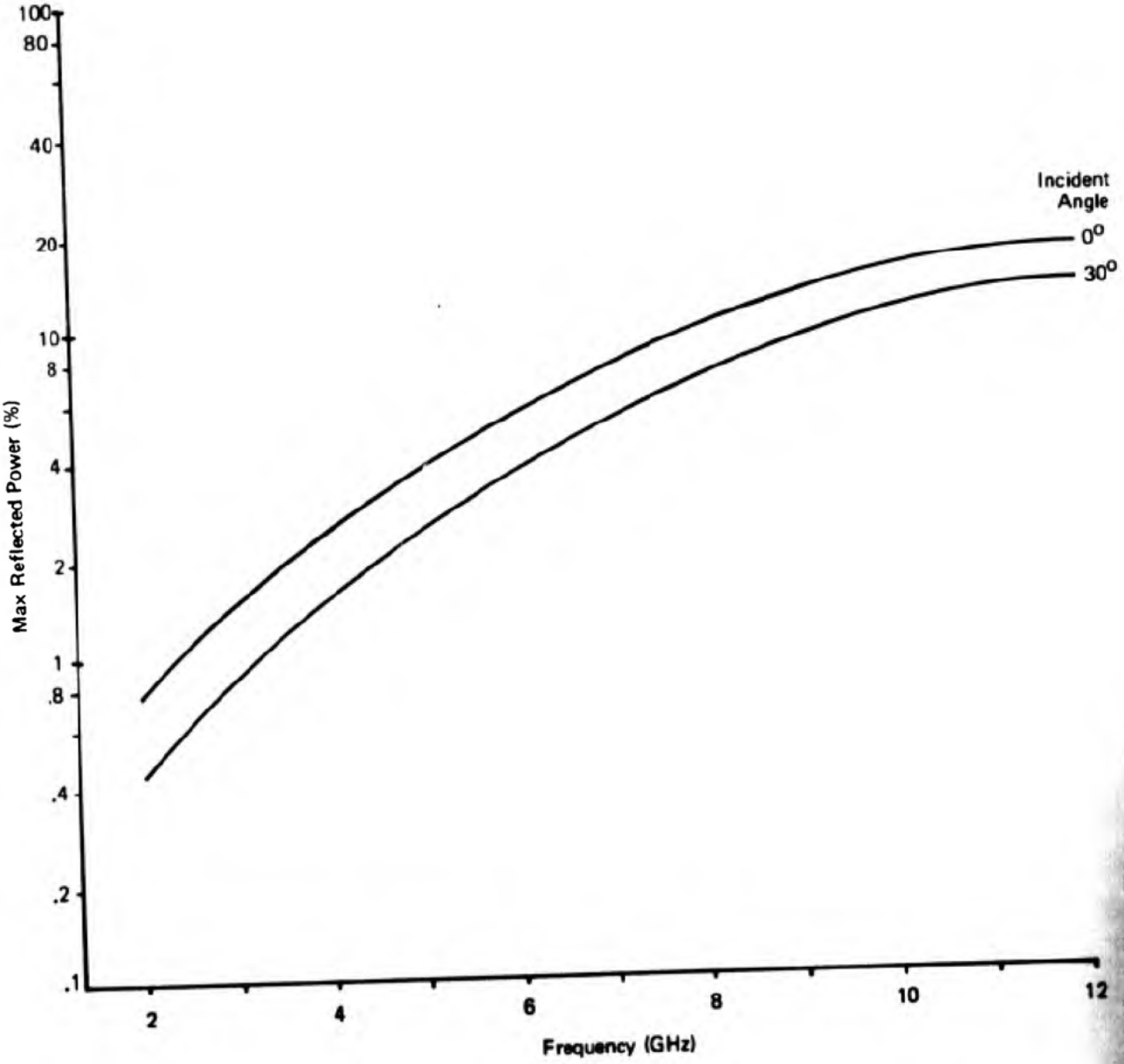

Figure 3.26: Reflected Power, .020-In. Skin Sandwich (U)

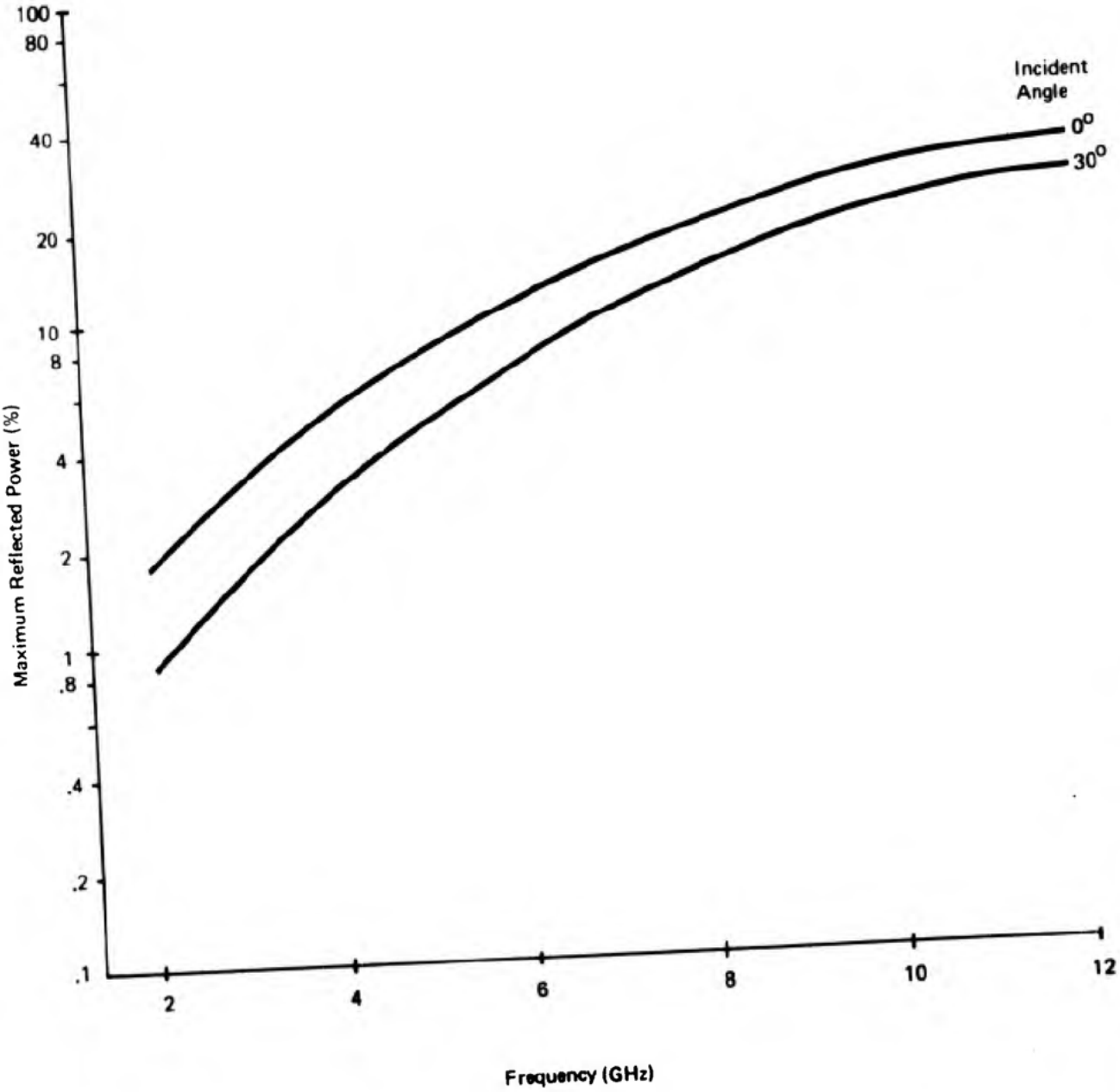

Figure 3-27: Reflected Power, .030-In. Skin Sandwich (U)

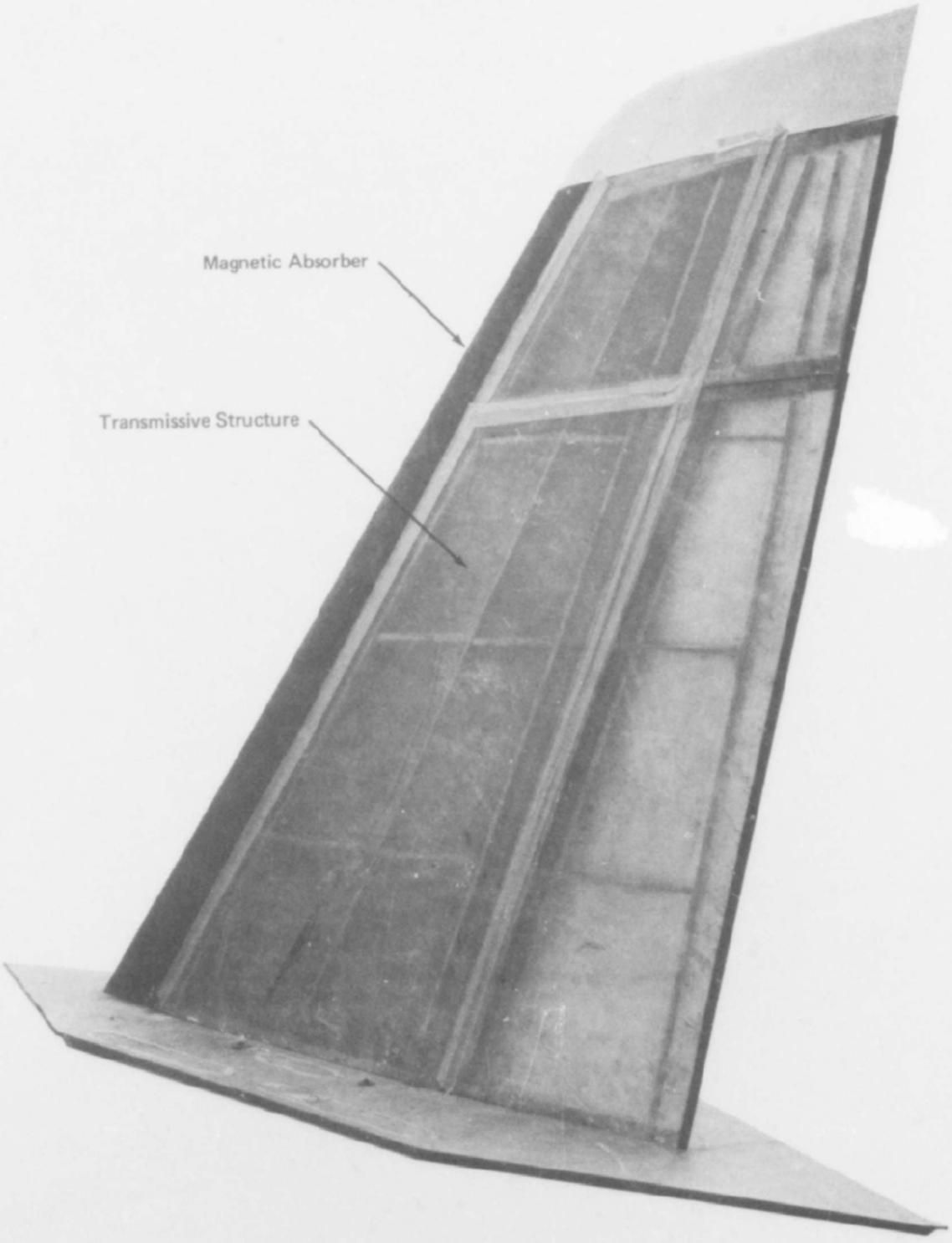

Figure 3.28: Transmissive Panel Installation (U)

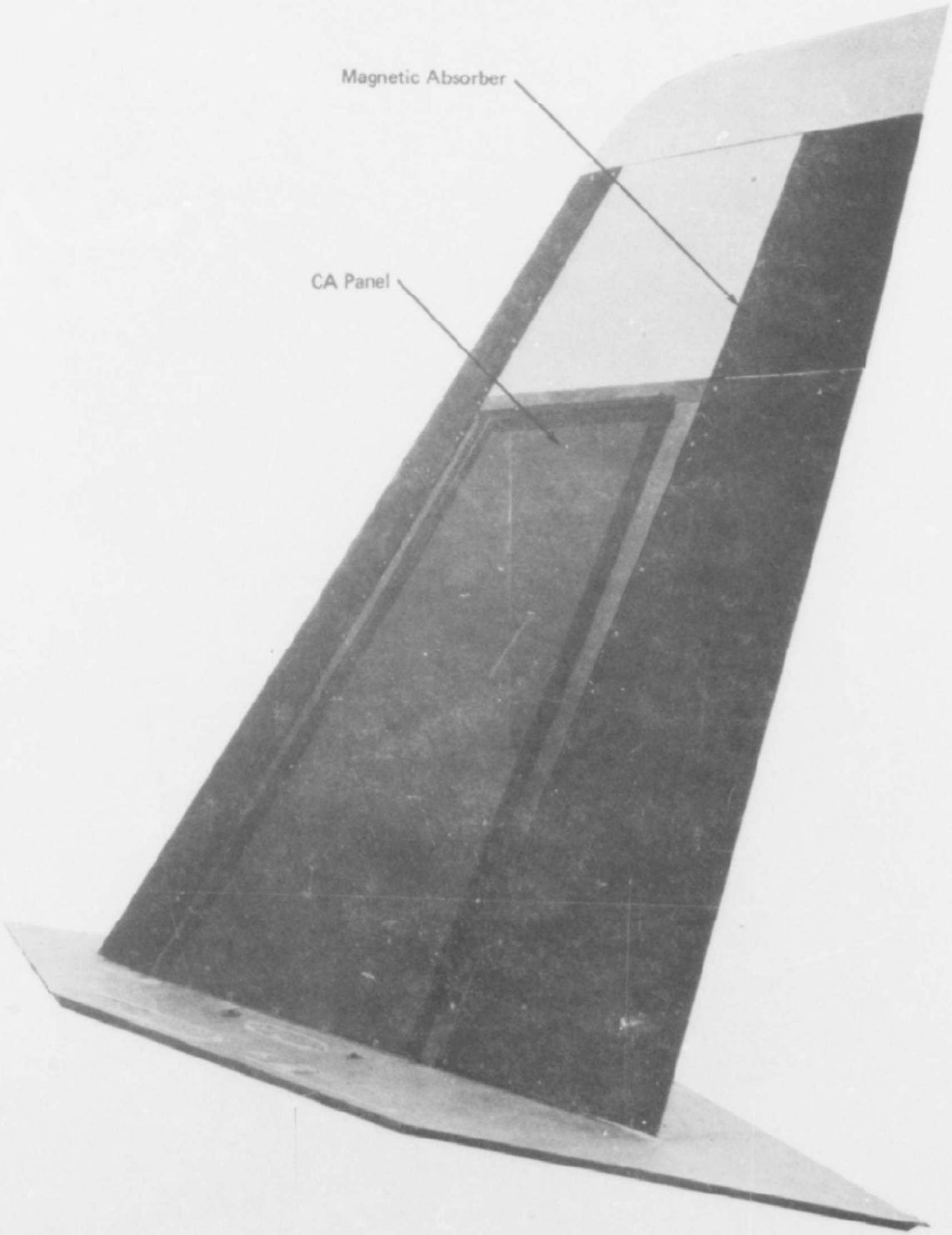

Figure 3.29: CA Absorber Installation (U)

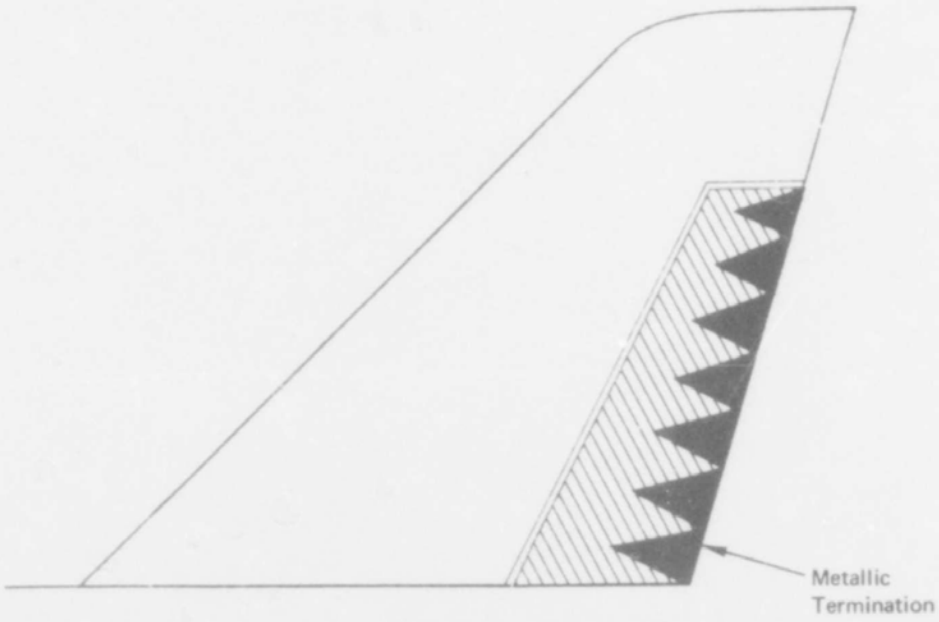

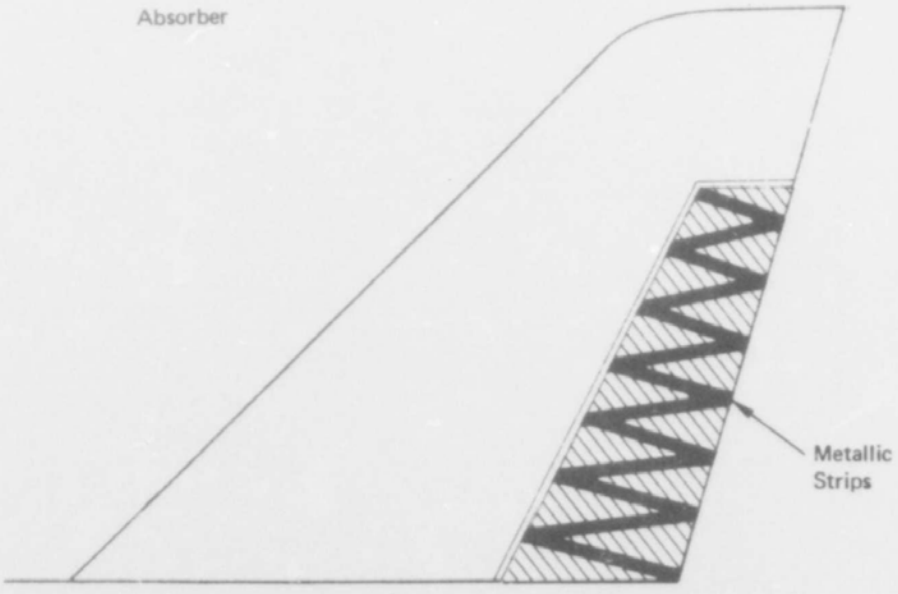

Figure 3.30: Trailing Edge Terminations (U)

angle tested (0, +10, +20 and +30 degrees) across the forward, aft and broadside sectors. An additional summary was performed by averaging the ten degree median values (in db relative to one square meter) for each sector and at each conic angle. These methods of summarizing the RCS data are used to illustrate trends but they also can hide some effects at particular test conditions or model orientation. Therefore, the individual measured data were relied on for the final analysis of the RCS reduction techniques.

(U) The RCS for each model configuration was analyzed for the forward and aft sectors combined, and the broadside sector separately. This was to isolate the influence of treatments to reduce broadside RCS on the fore and aft sector RCS.

3.4.1 Fore and Aft Sector RCS Data

(C) The results of the various tests made on the model and the RCS of the smooth model are shown in part in Figures 3.31, 3.32 and 3.33 for frequencies of 2, 4 and 10 GHz, respectively. These figures show the average of the ten degree median RCS over a +60° yaw sector from nose-on (fwd) and tail-on (aft) at both vertical and horizontal polarizations. Data is shown in Figure 3.31 at 2.0 GHz for the five model configurations listed in Table 3-1. The panel joins and rudder hinge gap were covered with metal tape for all the configurations except the baseline.

(C)

Configuration	RCS Reduction Applied
Baseline	No RCS treatment applied.
B	Absorber leading edge, transmissive side panels and rudder.
C	Absorber leading edge and rudder, transmissive side panels.
F	Absorber leading edge and rudder, circuit-analog RAM side panel (left side only).
I	Absorber leading edge and rudder, metallic strip rudder termination (Figure 3.22).
J	Absorber rudder, metallic strip rudder termination.

TABLE 3-1

(C) The dashed lines show the data for configurations F and J which represent the preliminary design configuration with and without broadside RCS control as discussed in Section 5.0. Configurations

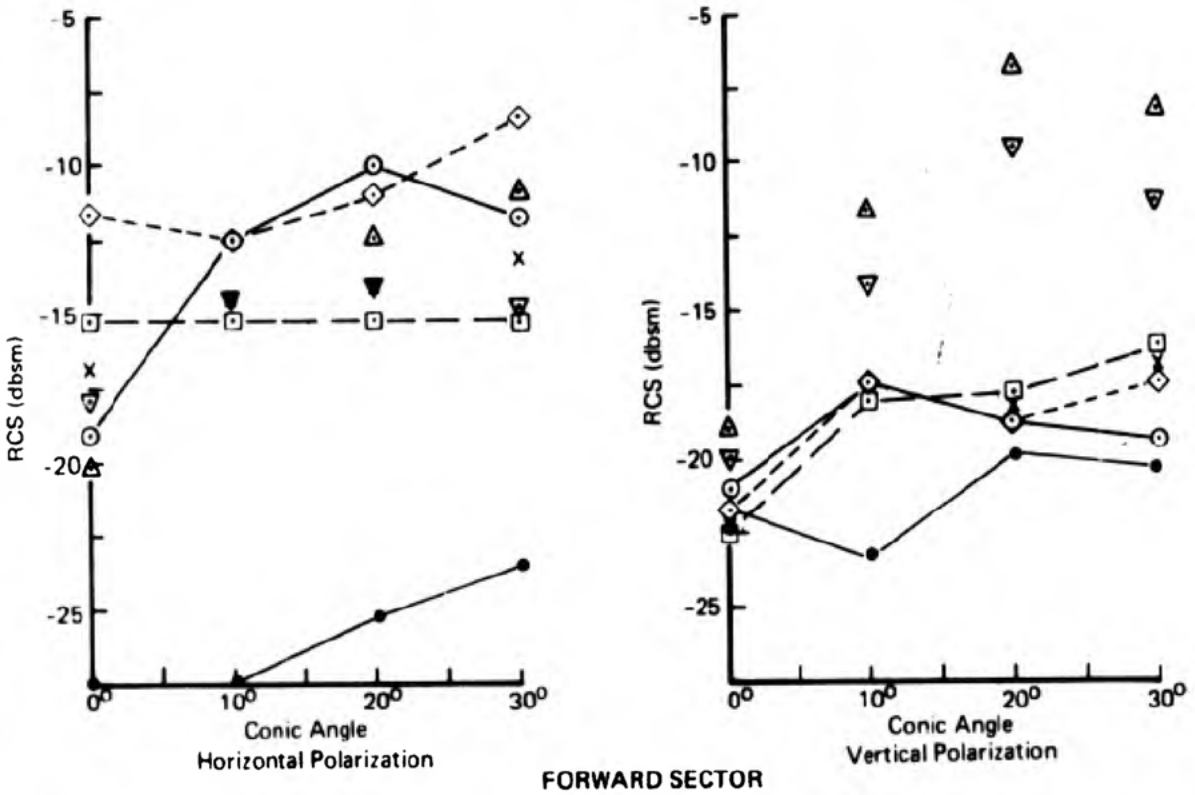

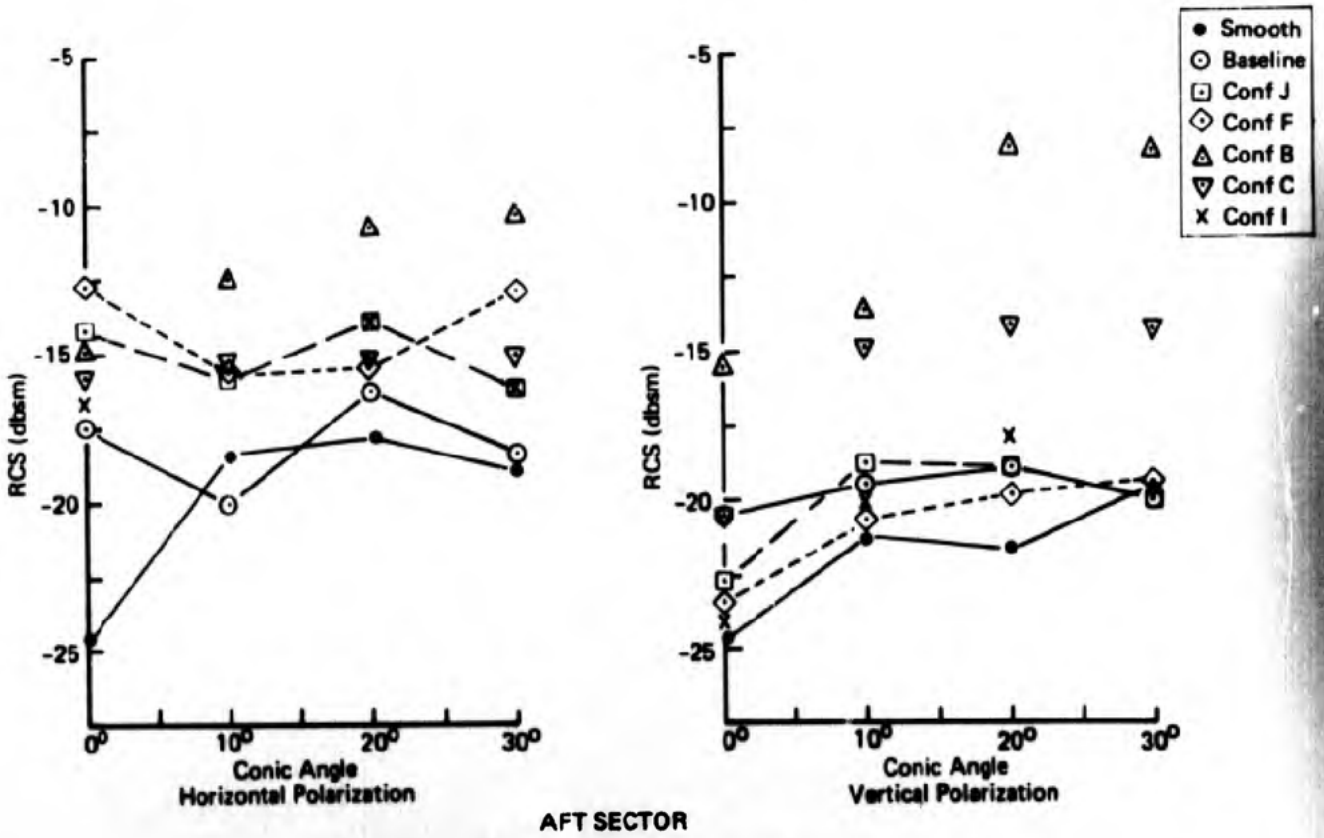

Figure 3.31: 2.0 GHz RCS (± 60° Average of 10° Medians) (U)

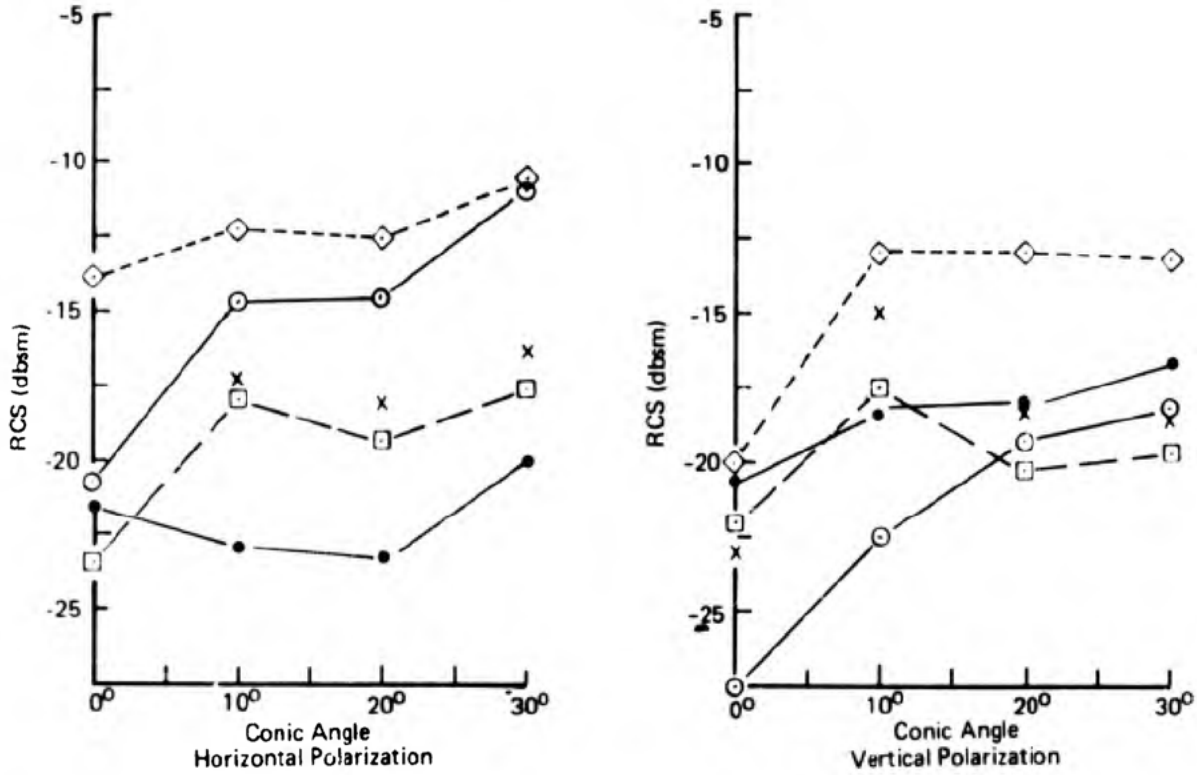

FORWARD SECTOR

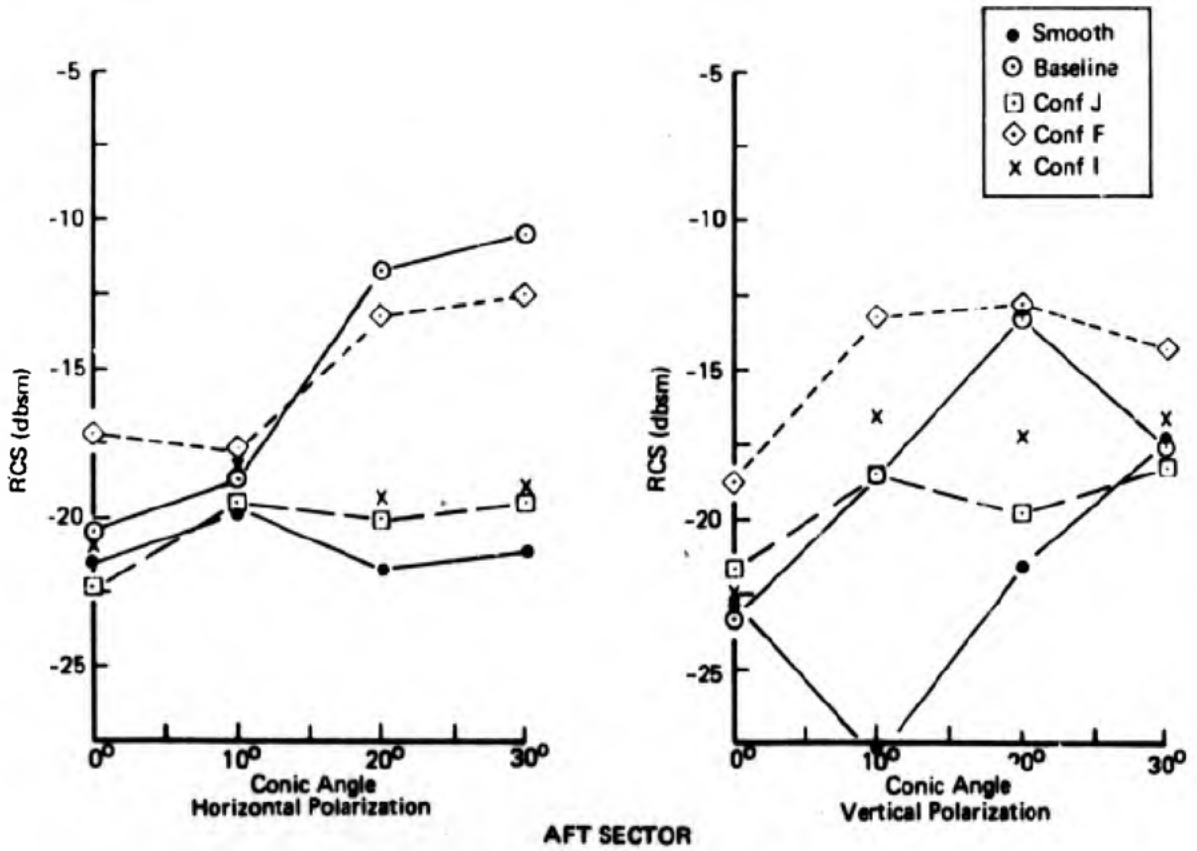

AFT SECTOR

Figure 3.32: 4.0 GHz RCS (± 60° Average of 10° Medians) (U)

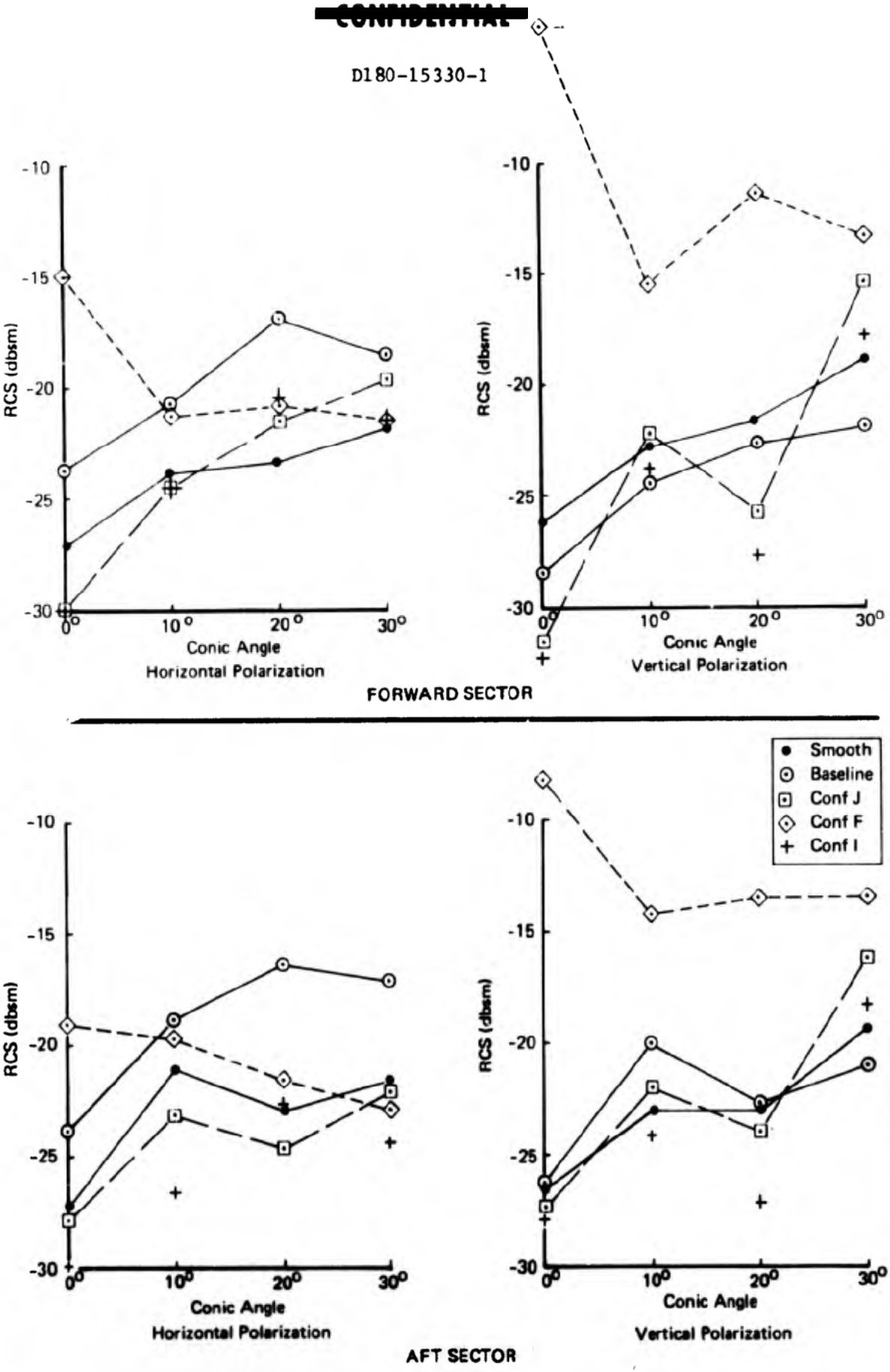

Figure 3.33: 10 GHz RCS (± 60° Average of 10° Medians) (U)

B and C (these incorporate transmissive side panels) were not tested at 4 and 10 GHz. The 2 GHz tests on configurations B and C show a substantial increase in nose and tail sector RCS. Furthermore, the prototype transmissive panels used for these tests were not stiff enough to support the model structure and the use of these panels for additional tests could jeopardize the model. The use of transmissive panels to control RCS is not excluded from consideration and is discussed in Section 4.0.

(C) The forward sector RCS for horizontal polarization was of primary concern at 2 GHz as the average over the sector reached 0.1 square meter at a 20° conic angle for the untreated tail. The forward and aft sector RCS at horizontal polarization were of concern at 4 GHz as they both approach 0.1 square meters. The 10.0 GHz RCS was not as high for the untreated model and therefore was of less concern.

(C) The absorber rudder and trailing edge (Configuration J) configuration shows a substantial decrease in RCS for the forward sector at horizontal polarization. Note that a 3 db decrease (factor of 2) in the average of the median RCS over a $\pm 60°$ sector usually indicates a much larger reduction in RCS at particular angles within the sector. This is illustrated in the curves of Figures 3.34 and 3.35. These curves show the ten degree median RCS at 2.0 GHz and 4.0 GHz for the untreated model and for configuration J.

(C) A substantial RCS reduction in the forward sector for horizontal polarization is noted for configuration J at 2 GHz. The vertical polarization shows some differences with the near nose-on and tail-on values lower for the J configuration whereas the opposite is true for the angles between 30° and 60°. The aft sector RCS at horizontal polarization is higher for configuration J at 2 GHz but below 0.1 square meters. This increase is due to the electrical discontinuity between the absorber and metal surfaces. The absorber installation was designed to provide as smooth a physical transition as possible but the prototype absorber structure did not include a suitable electrical transition. The required transition can probably be achieved by gradually tapering the absorber to a thin edge at the forward edge of the part. The design of suitable edge transitions is a subject worthy of additional study. This transition is critical to the travelling waves launched from near tail-on aspects and reflected at the metal-absorber join. Apparently the termination provided for travelling waves launched from near nose-on aspects is somewhat better judging by the lower RCS attained.

(C) The RCS reduction achieved by incorporating the absorber rudder and trailing edge surface is substantially improved at 4.0 GHz and at 10 GHz in both the forward and aft sectors. The ten degree median RCS at 4 GHz is shown in Figure 3.35. The measured RCS at 4 GHz horizontal polarization) is shown in Figure 3.36 to illustrate the substantial RCS reduction achieved at this frequency. The RCS at

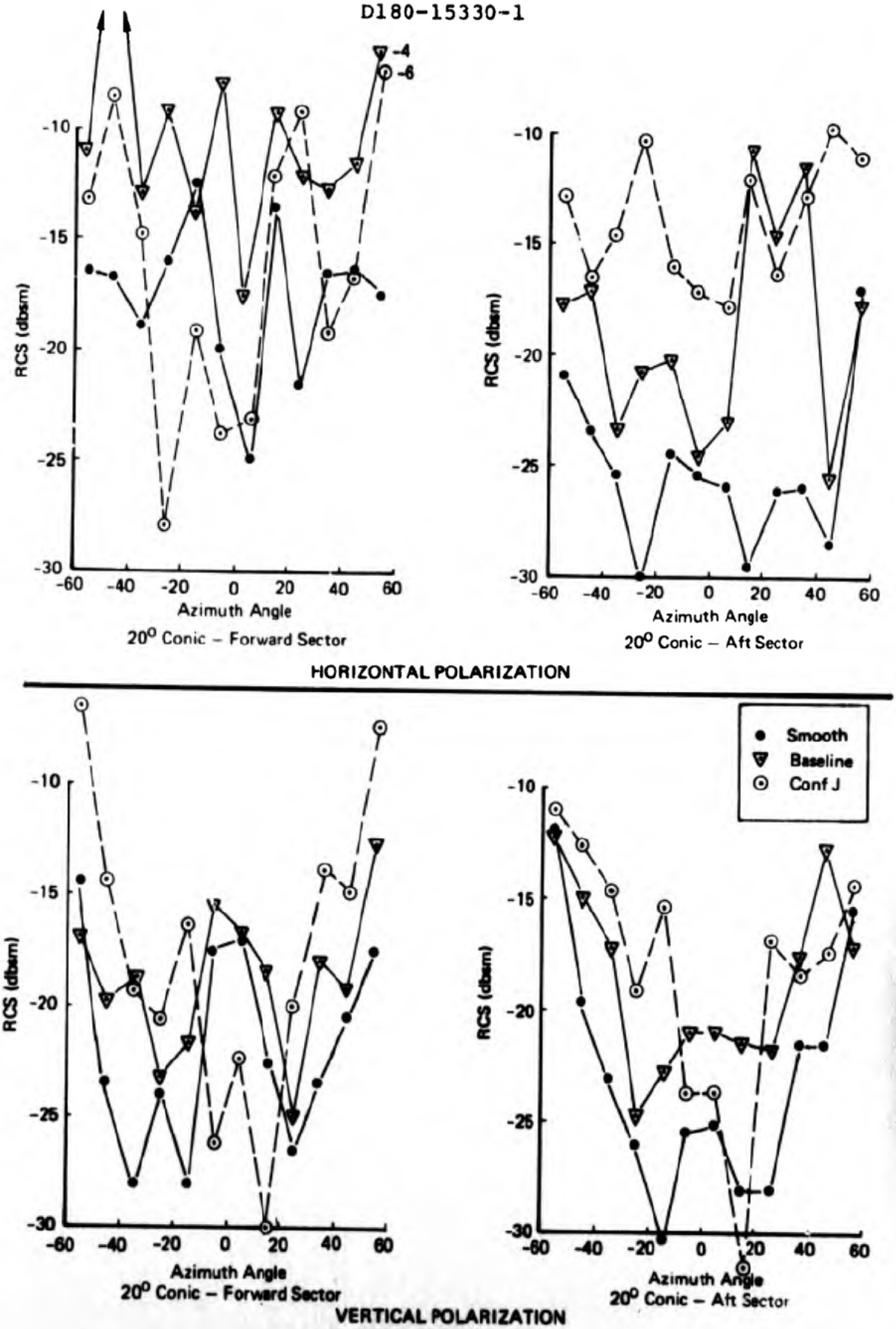

Figure 3.34: 2.0 GHz 10° Median RCS (U)

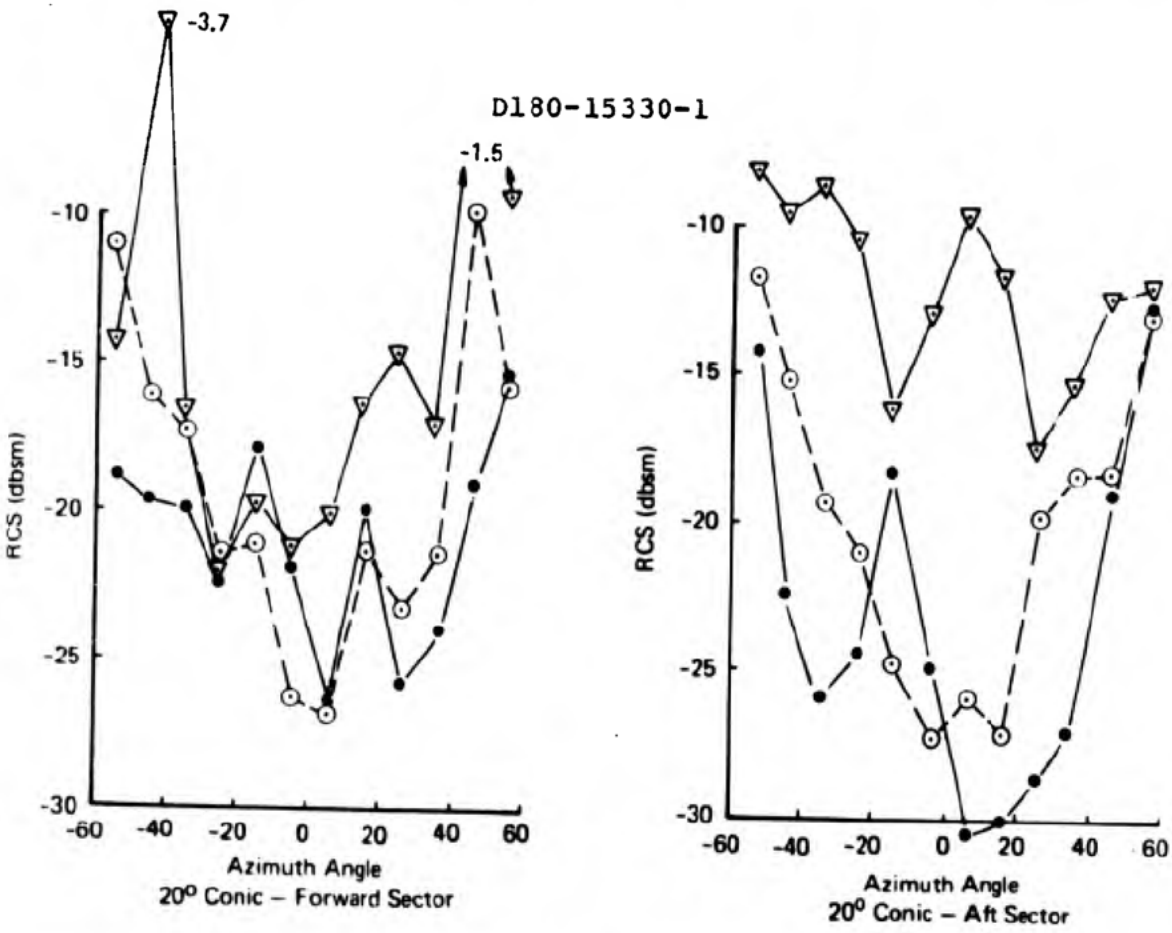

HORIZONTAL POLARIZATION

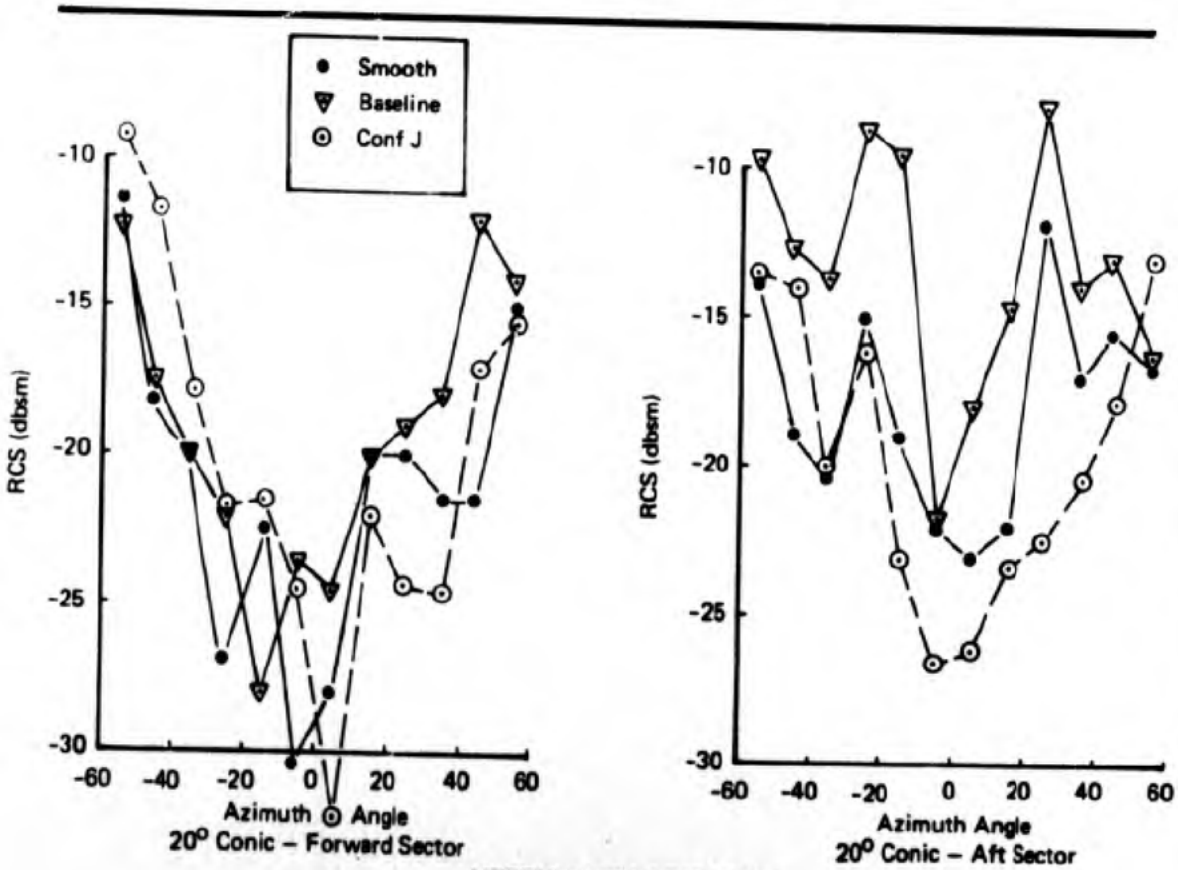

VERTICAL POLARIZATION

Figure 3.35: 4.0 GHz 10° Median RCS (U)

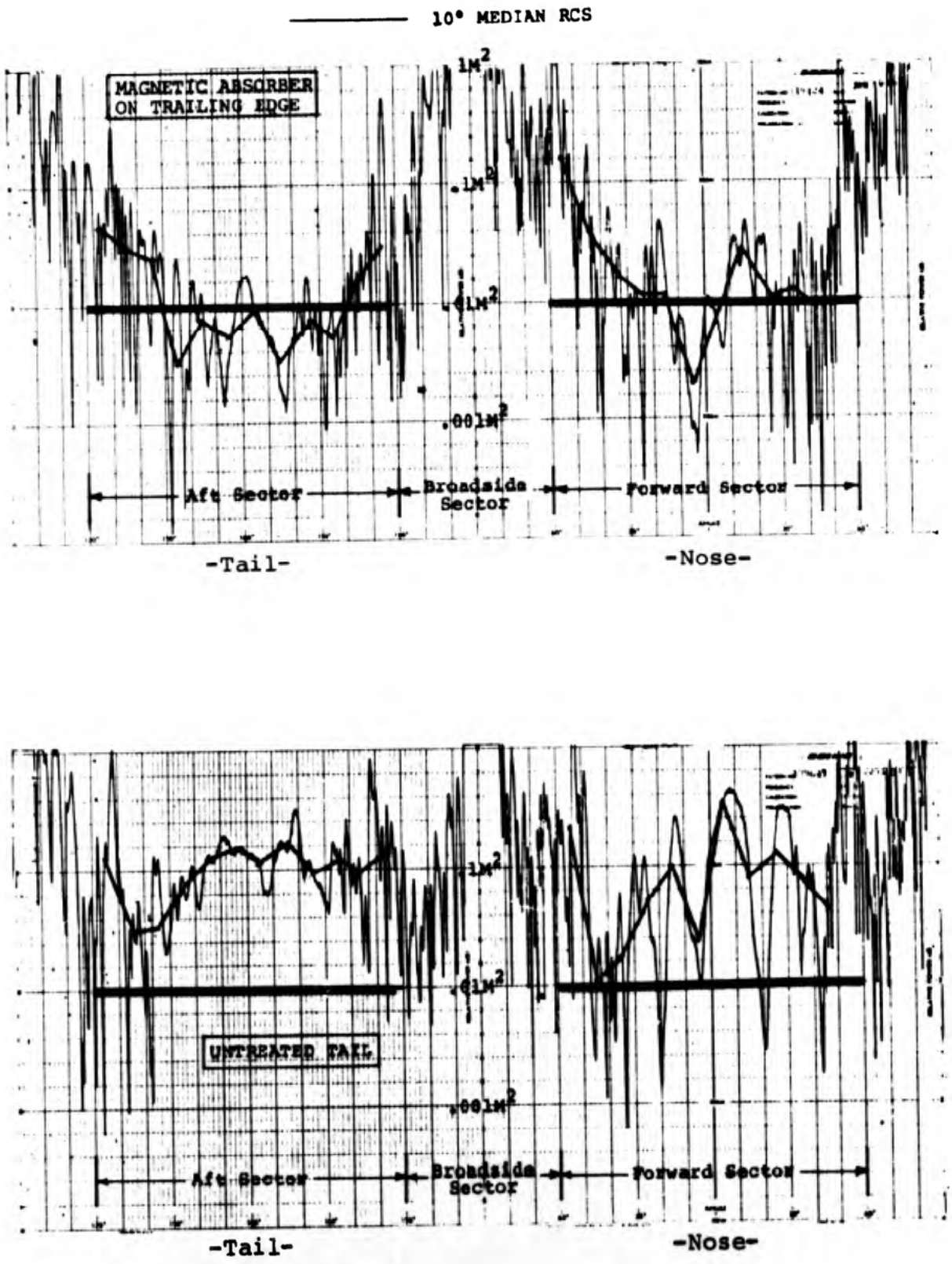

Figure 3.36: 4 GHz Vertical Tail Measured RCS – 30° Conic (U)

vertical polarization is increased at a +30° conic angle at 10 GHz compared to the untreated model. Again the absorber-metal join is felt to be responsible for this return.

(C) The effect of an absorber leading edge fairing in combination with the rudder and trailing edge treatment (Configuration I) was not substantial and was not included in the final preliminary design. The effect of this treatment can be seen by comparing the data from configurations I and J.

(S) The incorporation of the circuit-analog (CA) absorber on the left side of the model (Configuration F) provides for a substantial increase in the forward and aft sector RCS at 4.0 and 10 GHz. The increase at the lower frequencies is probably due to the physical discontinuties which are present for the test panels. The increase at 10 GHz is a phenomena associated with the CA absorber. These absorbers provide a large lobe, analogous to a grating lobe from array structures, at the upper microwave frequencies (above 9.0 GHz). This phenomena has been observed in previous tests and is a shortcoming associated with this type of absorber. The final preliminary design discussed in Section 4.0 shows a specular absorber installed on the side and leading edge of the tail to reduce the broadside sector RCS. The feasibility of developing a suitable absorber for this application which does not influence the forward and aft sector RCS can be best determined through additional study.

Broadside RCS

(C) The two techniques studied for control of the broadside RCS (transmissive and absorber panels) were designed to remove the large specular lobe from the tail at near broadside aspects. The reduction in the specular RCS is relatively straight forward, however the major difficulty is in maintaining the low forward and aft-sector RCS when incorporating the reduction techniques. Regarding the broadside RCS the transmissive panels are more effective at lower frequencies and the circuit-analog panels are more effective at the higher frequencies.

(S) In general these techniques provide for a 6-10 db reduction in the broadside RCS. The unreduced median RCS is about 100 square meters at broadside and can be reduced to 10 or 20 square meters depending on the frequency. The transmissive panels have an advantage in cost and weight over the circuit analog or multi-layer absorber panels. Unfortunately both techniques have shown adverse effects on the forward and aft sector RCS. Techniques for reducing these effects (such as shaping the internal spars and frames, or designing multi-layer absorber without the grating "lobes") are suggested but additional research into these problems are required.

4.0 LOW RCS TAIL-PRELIMINARY DESIGN

(S) The preliminary design for a low RCS tail is shown in Figure 4.1. Significant design features are:

1) The rudder and trailing edge is constructed of a nominal 0.10 inch thick fiberglass laminate with iron-loaded, epoxy resin matrix. The resin is an Emerson and Cumming CR-124 or equivalent.

2) The leading edges of the absorber laminate are tapered to a thin edge to provide an appropriate electrical transition.

3) All surface gaps and discontinuties are controlled and filled with an electrically conductive filler if required. A nominal .050 inch maximum surface discontinuity is assumed. This tolerance would be verified during design development.

4) The rudder hinge slot is covered with a flexible metal flap. This is tapered to provide a smooth transition onto the rudder surface. A rudder movement of +15 degrees has been assumed. The hinge flap geometry would be adjusted accordingly to provide for additional rudder movement.

5) A structural, multi-layer specular absorber construction is shown for the tail side and leading edge surfaces. This is an optional feature to control broadside RCS. The details of the absorber are not shown and would have to be developed. A conventional frame and skin construction with a metallic surface is recommended if no broadside RCS reduction is required.

(U) The use of this tail will influence airplane cost weight and aerodynamic drag as follows:

Cost

(C) The costs associated with the absorber laminates, hinge flap and surface finish control are very small. There will be some development costs but not significantly larger than the cost of developing conventional structure. Recurring costs are essentially identical to that of a conventional structure. The use of a structural absorber side panel will involve somewhat larger design and recurring costs. Past experience in these materials has shown that close tolerances are required and the costs are increased accordingly. However, based on previous studies the absorber costs will not be significant compared to the total airplane costs. Total cost differentials will be on the order of $1000 per aircraft.

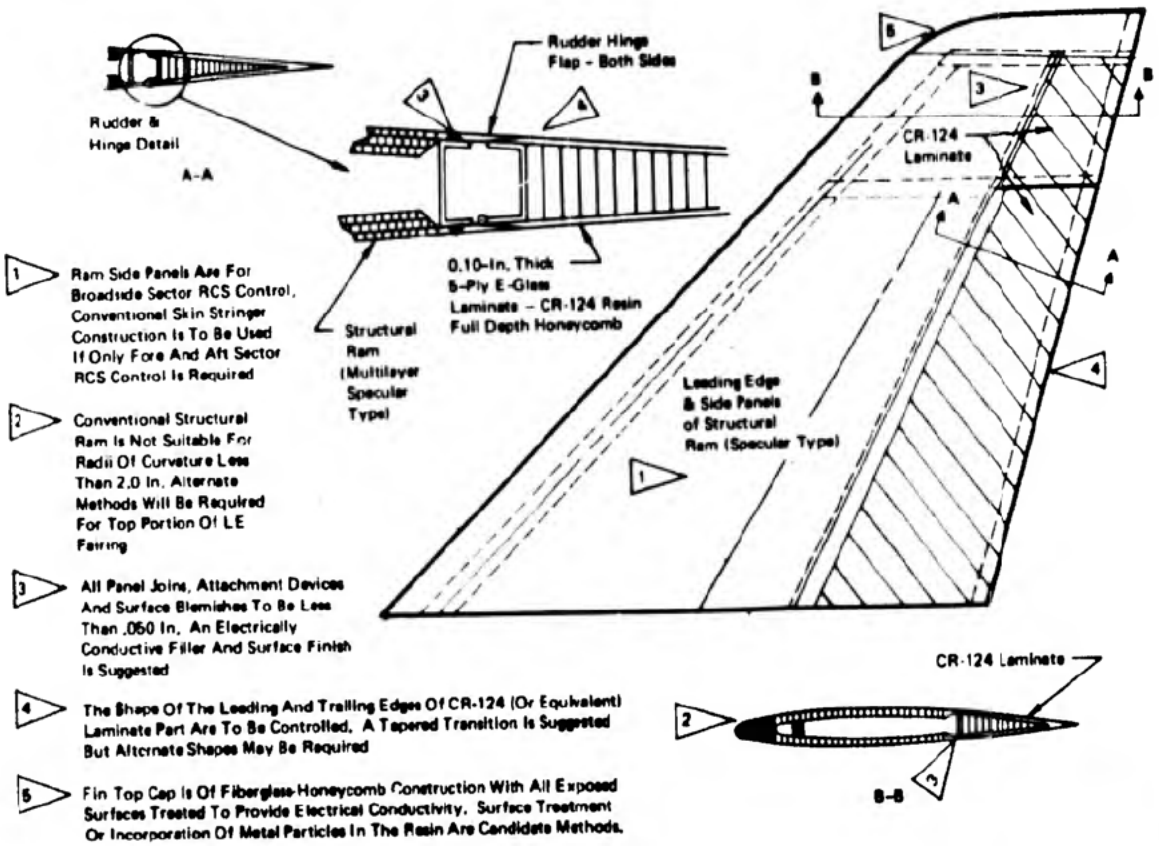

Figure 4.1: Low RCS Vertical Tail (U)

Weight

(C) The weight increase (compared to the conventional construction used for the baseline) associated with the absorber laminate parts will total about 50 lbs. for the tail. This assumes a 2.3 lb/ft^2 increase and is based on the weights of the test specimens built during this study. A lesser surface area treatment will possibly provide a comparable RCS with lesser weight. This would be determined during the design program.

(C) The structural absorber (if used) will also provide a 50 lb. increase in the weight of the tail assuming a 1 lb/ft^2 increase, typical of this type of material.

Aerodynamic Drag

(C) The rudder hinge flap and surface finish control will provide for a reduction in drag. The total drag reduction is probably not significant (depending on the total airplane drag) and can be ignored. The design shown will provide for a low-forward and aft-sector RCS (assuming the specular absorber is not included) at no significant cost or aerodynamic penalty. The weight increase shown (50 lbs) considers only the tail treatment. A total airframe treatment would likely result in a 200 lb. weight increase.

(C) This represents less than one percent of the total airplane gross weight (assuming a typical 25,000 to 50,000 lb. airplane) and the airplane can be sized to maintain mission performance with this weight increase. The optional feature of incorporating specular absorber for broadside RCS control has a small cost increase associated with it as well as providing another 50 lb. weight increase. Furthermore, the broadside RCS reduction which could be achieved (6-10 db) may compromise the forward and aft sector RCS. Shaping techniques combined with some absorber is considered a more practical solution to the broadside sector RCS problem.

5.0 TOTAL AIRFRAME RCS

(S) This program has been directed towards the analysis and control of the RCS from a vertical tail. The remaining control surfaces, horizontal tails, wings and other surfaces (canards, etc.) are similar and the results of this study will generally apply. The study has shown that the untreated vertical tail will provide an average RCS over the forward sector near 0.1 square meter. When the other control surfaces are considered it is likely that an average RCS near 0.5 or 1.0 square meter will result for many airplanes. Furthermore, at certain angles the ten degree median RCS can exceed 1.0 square meter from any one surface and the peak RCS can go as high as 10 square meters. If even moderate levels of RCS (1-10 square meters) are required the RCS from the control surfaces will be a major RCS contributor.

(S) The RCS reduction techniques developed during this study can (assuming a continuing design and development program) provide RCS levels below .01 square meters for the various control surfaces in both the forward and aft sectors. A total forward and aft sector airframe RCS near .01 square meters is felt to be realizable and practical based on these preliminary results.

(C) The results of this study clearly indicate that treatments to reduce the broadside sector RCS must consider travelling wave reflections to maintain a low RCS in forward and aft sector as well. At this time shaping of the airframe in conjunction with absorbers or other treatments appears to be the most effective approach to control of the RCS in the broadside sector. This also will have to be substantiated with additional research. Broadside sector RCS control has not been explored in a thorough comprehensive manner for any but a few specialized aircraft. Therefore there are numerous unresolved questions as to how to control the RCS in the broadside sector.

(C) The analysis and test results presented in this report are directly applicable to any type of control surface. Furthermore, this program has provided for confidence that the forward and aft sector RCS from control surfaces can be effectively reduced.

6.0 CONCLUSIONS

(U) The analysis of the results of this program has led to several conclusions relevant to the RCS and the RCS reduction of aircraft control surfaces. These conclusions have been verified by experiment and are applicable to control surfaces in general.

(S) 1) The control surfaces can provide a RCS which can approach 0.5 to 1.0 sq. meters in the forward and aft sectors. This contribution is predominately from travelling waves and has not been accounted for in prior airplane RCS studies.

(U) 2) The travelling wave RCS contribution is primarily due to near planar surfaces. Curved surfaces will not provide substantial travelling wave backscatter.

(S) 3) The travelling wave RCS for control surfaces is predominate for the low to mid-band microwave frequencies (about 2-8 GHz). At higher frequencies the RCS from travelling waves are confined to very narrow angular regions and the airplane surfaces are more curved (relative to the radar wavelength), reducing the backscattered travelling waves.

(S) 4) The RCS from the control surfaces can be reduced to a level of below .01 square meters in the forward and aft sectors, by "smoothing" all surface discontinuties, incorporating absorber for abrupt edge terminations (noteably trailing edges) and by appropriately shaping all metal - absorber transitions.

(S) 5) The broadside sector RCS can be reduced by about a factor of 4 (-6 db) using either absorber or transmissive structure. This can increase the RCS in the forward and aft sector unless suitable edge transitions and/or internal structure treatments are provided.

(C) 6) Absorber structure suitable for attenuation of travelling waves can be provided using a laminate of fiberglass with an epoxy matrix loaded with a suspension of magnetic particles. This absorber can be designed to provide a significant normal incidence (plane wave) attenuation.

(U) These conclusions are derived from the results of the studies conducted during this program. The program has successfully identified the nature and extent of the RCS for control surfaces, developed RCS reduction techniques for these surfaces and established requirements for further study (described in Section 7.0). The program has provided preliminary understanding of the backscatter from airplane control surfaces.

7.0 RECOMMENDATIONS

(U) There have been several technical questions raised as a result of the studies conducted during this program. The resolution of these questions is necessary to achieve a sound technical basis for attaining low RCS for aircraft. Therefore, the following recommendations for additional research are provided in order to identify those areas where technology deficiencies exist and to propose an approach to remove each of these deficiencies.

(C) 1) Broadside Sector RCS Control

The incorporation of techniques to reduce the broadside sector RCS made during this study showed a substantial increase in the forward and aft sector RCS. The techniques studied included both transmissive and absorptive structures. Additional studies are required to explore broadside RCS reduction techniques which are compatible with low RCS in the forward and aft sectors.

(U) 2) Travelling Wave RCS

The nature of travelling waves was explored on a preliminary basis using a semi-emperical approach during this program. A more thorough study which would develop a theoretical description of the travelling waves, with experimental verification is required. The study should examine the effects of surface roughness, shape and edge terminations. In addition, the inclusion of dielectric and/or magnetic materials along and adjacent to a metallic surface should be studied. The launching mechanism for travelling waves should also be examined and include radius of curvature and edge shape. The study would provide a more precise theoretical description of the RCS due to travelling waves and a basis for the design of treatments to reduce the RCS from the surface details (small gaps, absorber edges, etc.).

(C) 3) Magnetic Absorber Structure

The use of a magnetic structural absorber has been demostrated during this program. However, the improvements in electrical and structural performance which can be realized for this type of material should be examined further. The design of this type of material to attenuate both travelling waves and the near-normally incident plane waves should be studied. The influence of shaping the material and combining the magnetic laminates with other absorbers should be established. This type of material is particularly suited to aircraft applications where very low RCS is required. In general these recommended studies are necessary if levels of RCS below 1 square meter are required.

REFERENCES

1. Ross, R.A., "Radar Cross Section of Rectangular Flat Plates as a Function of Aspect Angle", IEEE Transactions, Antennas and Propagation, May, 1966.

2. Peters, L., End-Fire Echo Area of Long Thin Bodies, The Ohio State University Research Foundation, Report No. 601-9 (June, 1956), AF 33(616)2546, AD 100980.

3. Peters, L., End-Fire Echo Area of Long Thin Bodies, Trans. IRE AP-6: 133(1958).

4. Peters L., Echo Area Properties of Bodies Due to Certain Travelling Wave Modes, The Ohio State University, Research Foundation, Report No. 777-19 (May 1960).

5. Ruck, G., et al, Radar Cross Section Handbook, Volumes 1 and 2, Battelle Memorial Institute Columbus Laboratories, Plenum Press, 1970.

DISTRIBUTION LIST FOR TECHNICAL REPORT #1

	No. of Copies
Office of Naval Research Department of the Navy Arlington, Virginia 22217	
ATTN: D.S. Siegel, Code 461	4
Dr. A. Shostak, Code 427	1
Director U.S. Naval Research Laboratory Washington, D.C. 20390	
ATTN: Code 5340	1
Tech Info Division	1
Chief of Naval Operations Washington, D.C. 20350	
ATTN: NOP-382E2	1
Chief of Naval Material Washington, D.C. 20360	
ATTN: NMAT 0334	1
Commander Naval Air Systems Command Washington, D.C. 20361	
ATTN: NAVAIR 310B	1
NAVAIR 320A	1
NAVAIR 320B	1
NAVAIR 370S	1
NAVAIR 510A3	1
NAVAIR 52033B	1
Director Office of Naval Research Branch Office 1030 East Green Street Pasadena, California 91101	
ATTN: CDR R.L. Brekon	1
Mr. R.F. Lawson	1
Air Force Avionics Laboratory Wright Patterson AFB, Ohio 45433	
ATTN: WRP (W. Bahret)	1
WRD (T. Madden)	1
Air Force Flight Dynamics Laboratory Wright Patterson AFB, Ohio 45433	
ATTN: FSB (D.W. Voyles)	1
PTS (D. Fearnow)	1
PTR (J. Seaburg)	1

DISTRIBUTION LIST FOR TECHNICAL REPORT #1 (CONT)

	No. of Copies
Headquarters U.S. Air Force Washington, D.C. 20330 ATTN: AFRDRE	1
Commander Naval Air Development Center Warminster, Pa. 18974 ATTN: Dr. G.L. Hollingsworth Code 01	1
J. Guarini Code AER-3	1
Defense Documentation Center Cameron Station, Building 5 5010 Duke Street Alexandria, Virginia 22314	2
Air Force Materials Laboratory Wright Patterson AFB, Ohio 45433 ATTN: LTF (S. Litvak)	1
LPT (R. Van Vliet)	1
LAE (T. Reinhart)	1